American Mineralogist, Volume 71, pages 501–517, 1986

Fractionation trends of the Nb- and Ta-bearing oxide minerals in the Greer Lake pegmatitic granite and its pegmatite aureole, southeastern Manitoba

PETR ČERNÝ, BRUCE E. GOAD,[1] FRANK C. HAWTHORNE, RON CHAPMAN
Department of Earth Sciences, University of Manitoba, Winnipeg, Manitoba R3T 2N2, Canada

ABSTRACT

The Greer Lake pegmatitic granite and related exterior rare-element pegmatites of the beryl-columbite type intrude metabasalt and tonalite gneiss in the Archean English River Subprovince of southeastern Manitoba. Columbite-tantalite is the predominant Nb- and Ta-bearing mineral, associated with subordinate ixiolite, microlite, niobian-tantalian rutile, and rare tantalian cassiterite, wodginite, and ilmenite. In coexisting mineral pairs, Ta/(Ta + Nb) of microlite exceeds that of columbite-tantalite, ixiolite, rutile, and cassiterite; in cassiterite and rutile, Ta/(Ta + Nb) is higher and Mn/(Mn + Fe) lower than in columbite-tantalite and ixiolite.

In Li-, Rb-, Cs-, and F-poor environments, limited Mn enrichment accompanies the fractionation of Ta, which culminates in ixiolite and subordinate microlite. In Li-, Rb-, Cs-, and F-rich parageneses, extensive Mn enrichment precedes the main Ta fractionation, which subsequently generates near-end-member manganotantalite, wodginite, and microlite. The Greer Lake and other fractionation trends indicate that a late-stage F-rich environment promotes extreme Fe/Mn fractionation prior to the main stage of Nb-Ta separation. The abundances of Sn, Ti, and Sc are not related to fluorine or rare-alkali enrichment, but increase from pegmatitic granite to pegmatites. The relative accumulation of Ti and Sc in the pegmatite aureole seems to be due to internal fractionation rather than assimilation.

Columbite-tantalite in the pegmatitic granite shows an intermediate to near-ordered structural state, but is highly disordered in the pegmatite veins. Crystallization in the disordered state is suggested, with subsequent ordering in slowly cooling granite but thermal quenching in the exterior pegmatites. However, the increase in Ti, Sn, Sc, and Fe^{3+} in the Nb- and Ta-bearing minerals of the pegmatite aureole may also have retarded ordering.

INTRODUCTION

Paragenetic and geochemical relationships among Nb- and Ta-bearing minerals from cogenetic granite-pegmatite suites are the most poorly documented and least understood aspects of this mineral family. Despite recent work on the compositional and structural variability of these species (Foord, 1982; Černý and Ercit, 1985), the geochemical features of their evolution in differentiating residual granitic magmas are obscure. Early work lacks specific data and tends to be oversimplified (Ginsburg, 1956; Beus, 1960; Solodov, 1971; Kuzmenko, 1978). More recent studies on the regional mineralogy of pegmatite fields and provinces generally lack information on the behavior of the Nb- and Ta-bearing phases in different pegmatite types and on their individual fractionation paths (Sahama, 1980; Wang et al., 1981; v. Knorring and Fadipe, 1981). The only exceptions are studies dealing with individual pegmatites and restricted groups of cogenetic veins (Černý and Turnock, 1971; Grice et al., 1972; Foord, 1976; Lahti, 1984; v. Knorring and Condliffe, 1984; Lumpkin et al., 1986), but even here the available information is often sketchy.

The present paper is the first in a series of comprehensive studies, conducted at our department, dealing with the paragenetic and geochemical evolution of Nb- and Ta-bearing minerals in geologically defined and petrologically well-characterized pegmatite sequences. The general research program is based on the development of reliable standards and procedures for electron-microprobe analysis (Ercit, 1986) and on extensive field work (Anderson, 1984; Ferreira, 1984; Goad, 1984; Paul, 1984; Wise and Černý, 1984a; Černý et al., 1985b; Ercit, 1986; Černý and Ercit, 1985; M. A. Wise, unpub. ms.). The present study utilizes some of the early results of Černý and Turnock (1971), but it is based mainly on Goad's (1984) thesis derived from field and laboratory studies terminated in 1979 and on extensive additional sampling and laboratory work conducted by the other authors in 1979–1984.

[1] Present address: 11151 Kingsbridge Drive, Richmond, British Columbia V7A 4T1, Canada.

0003–004X/86/0304–0501$02.00

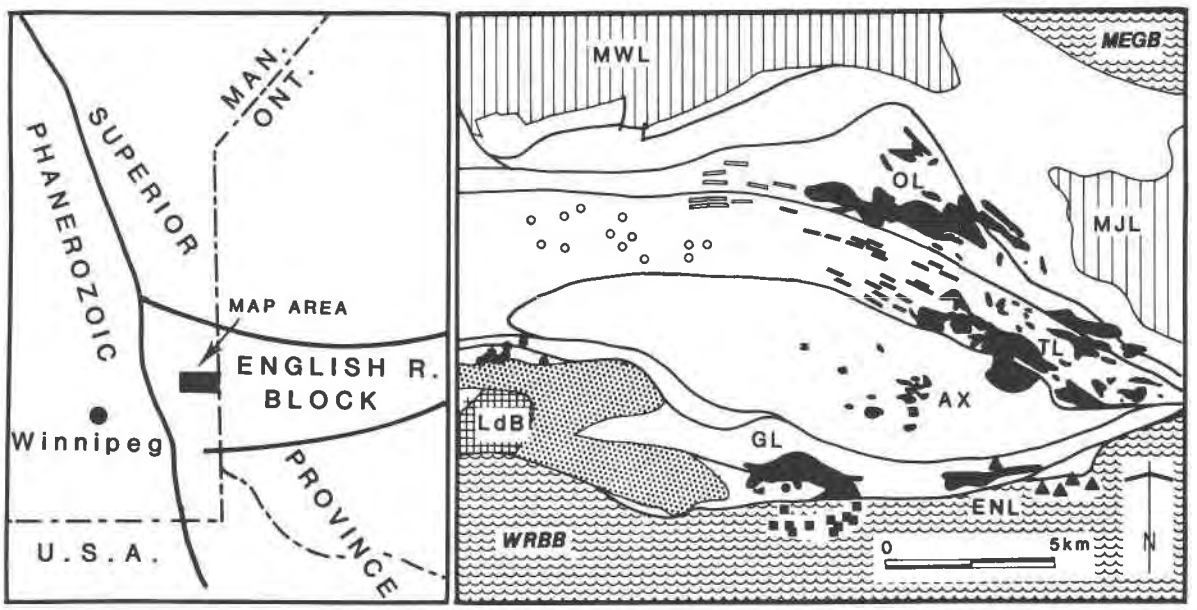

Fig. 1. Location of the study area and its geology: Bird River Greenstone Belt (open) between the Winnipeg River Batholitic Belt (WRBB) and the Manigotagan–Ear Falls Gneiss Belt (MEGB); Maskwa Lake (MWL) and Marijane Lake (MJL) tonalitic diapirs, eastern end of the complex Lac du Bonnet batholith (LdB). Most pegmatite groups (each marked by different spot symbol) are associated with pegmatitic granites (black; GL, ENL, AX, OL, and TL). Modified from Černý (1982).

Greer Lake granite and its pegmatite aureole

Location and regional geology

Greer Lake is located 135 km east-northeast of Winnipeg, at lat 50°20′39″N, long 95°19′W (Fig. 1). The pegmatitic granite and its pegmatite aureole are part of the Cat Lake–Winnipeg River pegmatite field situated in the westernmost English River Subprovince of the Superior Province (Černý et al., 1981a). The Bird River Greenstone Belt, host of the pegmatite field, consists of six formations of metavolcanic and largely related metasedimentary rocks of the Rice Lake Group, which form a broad and complex synclinorium (Trueman, 1980). Two major episodes of folding affected the greenstone belt; the second correlates with the diapiric intrusion of the Maskwa Lake and Marijane Lake batholiths and with the peak of the regional metamorphism. Metamorphism attained the greenschist-facies level over most of the map area of Figure 1 but reached amphibolite grade in its eastern and northeastern parts. Rb-Sr isochron dating of regional metamorphism and igneous activity places the regional evolution in the Kenoran orogeny (2.7–2.55 Ga; Černý et al., 1981a).

The dominant tonalite and trondhjemite components of the Maskwa Lake and Marijane Lake diapirs are rimmed and penetrated by largely undeformed biotite granites. The Lac du Bonnet batholith consists predominantly of an analogous late biotite granite, but an early and strained leucogranite constitutes its eastern extremity (Fig. 1) and irregular areas along its margin to the west. The leucogranite phase is alaskitic and highly fractionated; geochemical characteristics indicate that it is compositionally related to the late pegmatitic granites to the east and northeast.

Greer Lake pegmatitic granite

The Greer Lake intrusion is the southwestern one among the five pegmatitic granites of the Winnipeg River district that were emplaced along subvertical faults and adjacent décollement structures late in the history of regional events (Fig. 1; Goad and Černý, 1981; Longstaffe et al., 1981; Černý et al., 1981a). It is hosted largely by metabasalt. At the eastern and western extremities of the intrusion and at its southwestern offshoot, the contacts trend north at high angle to the layering and foliation of the metabasalts. These contacts are sharp, truncating both the layering and foliation with no evident deformation. Host-rock inclusions are rare in the pegmatitic granite, except for angular blocks of metabasalt in the southwestern offshoot indicative of stoping. A fault, striking west-northwest and transecting the Greer Lake intrusion, displays subvertical movement and separates the granite into two segments (Fig. 2). It seems likely that the pegmatitic granite is also truncated by a fault marking the boundary between the Bird River Greenstone Belt and the Winnipeg River Batholithic Belt (Figs. 1, 2).

The pegmatitic granite is compositionally and texturally heterogeneous: (1) pegmatitic leucogranite is dominant, consisting of megacrystic microcline-perthite (5–100 cm in size) intergrown with graphic quartz and embedded in a coarse-grained matrix of albite, quartz, and muscovite, with or without garnet; (2) fine-grained, massive, and homogeneous leucogranite is an equigranular facies consisting of microcline perthite, quartz, albitic plagioclase, and muscovite, with accessory garnet and zircon; (3) sodic aplite typically consists of albite, quartz, muscovite, and garnet, with accessory apatite, gahnite, monazite, and opaque minerals; it is commonly layered with prominent bands of garnet; (4) potassic pegmatite layers alternate with aplite or reside in the pegmatitic leucogranite; they consist of graphic to blocky microcline-perthite and quartz, commonly in concentrically zoned patterns, locally with cleavelandite and muscovite, accessory beryl, garnet, cordierite, columbite-tantalite, and extremely rare apatite.

All four phases of the pegmatitic granite are highly fractionated: average data for five samples of the fine-grained leucogranite show K/Rb 87, K/Cs 5100, K/Ba 767, Ba/Sr 7.4, Rb/Sr 32.1, Mg/Li 4.7, Al/Ga 1526, and Zr/Hf 48.3. The potassic pegmatite is the most fractionated phase with K/Rb 28, Rb/Sr 56.5, Mg/

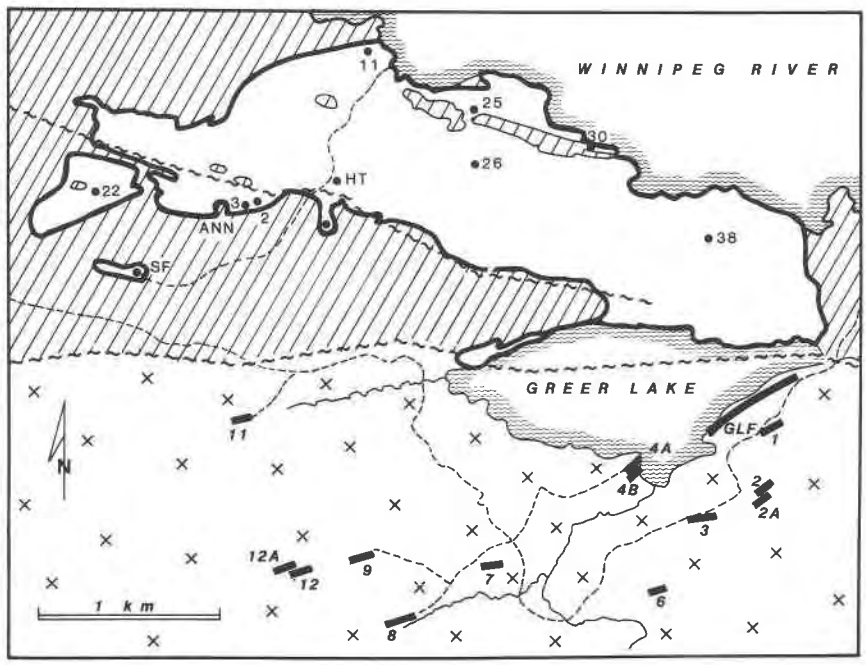

Fig. 2. The Greer Lake pegmatitic granite (open, heavy outline) in metabasalt (ruled) and the GL pegmatites (heavy bars in the gneissic terrane (X) south of east-trending fault. An east-southeast-trending fault separates the southwestern segment of the pegmatitic granite from its main body (GRS and GRN, respectively). Locality symbols mark the occurrences of Nb- and Ta-bearing minerals in the pegmatitic granite and the pegmatite veins (italics; cf. Table 1). Compiled from Černý and Turnock (1971) and Goad (1984).

Li 2.8, Zr/Hf 5.0, and Al/Ga 778. The southwestern segment of the intrusion is more fractionated than the main part north of the fault. It also hosts three highly fractionated pegmatite pods, the Annie Claim no. 2 and no. 3 and the Silverleaf Claim offshoot (Fig. 2).

Annie Claim no. 2 is an irregular pod of blocky microcline-perthite and quartz with abundant cleavelandite, several generations of Li-enriched micas, beryl, wodginite, and manganotantalite. The Annie Claim no. 3 is a subellipsoidal pod, highly enriched in Li, Rb, Cs, Mn, Be, Nb, Ta, and F. K-feldspar is extremely rare; lithian muscovite and lepidolite are the dominant potassic phases and are associated with quartz, albite, cesian beryl, and rare tourmaline, manganotantalite, microcline, apatite and cassiterite. Both AC2 and AC3 evolve from the surrounding pegmatitic leucogranite through a narrow transitional zone. In contrast, the Silverleaf offshoot consists largely of garnetiferous aplite with a large rounded pod of Li-, Rb-, Mn-, Nb-, Ta-, Be-, Sn- and F-rich pegmatite. The pod consists of microcline-perthite, quartz, albite, lithian muscovite, lepidolite, spessartine, cesian beryl, petalite, spodumene, topaz, cassiterite, manganocolumbite-manganotantalite, triphylite-lithiophilite, and amblygonite-montebrasite, with rare apatite, tourmaline, and sphalerite. Fractionation levels of all three pods are much more advanced than those of the potassic pegmatite units: blocky K-feldspar reaches K/Rb 10, K/Cs 139, and Rb/Cs 14, and some of the lithian micas have K/Rb 3, K/Cs 60, Rb/Cs 4.2, and Mg/Li 0.01.

These pods emphasize the overall highly fractionated nature of the southwestern segment of the pegmatitic granite, located in the wedge-shaped block between two prominent faults. In contrast, the potassic pegmatite phase of the less fractionated northern part of the pegmatitic granite closely resembles the predominant type of Greer Lake pegmatites hosted by the gneissic terrane south of the southern fault (Fig. 2). Thus it seems probable that the geochemically more primitive Greer Lake pegmatites in the south, and the main body of the pegmatitic granite in the north, are uplifted relative to the intervening greenstone wedge that hosts the more evolved granite segment.

Greer Lake pegmatite group

The Greer Lake pegmatites are dominantly concordant intrusions, pinching and swelling within the foliation of the hosting tonalitic and granitoid gneisses, both along strike and downdip. Typical dimensions of the pegmatite outcrops are well under 100 × 10 m; the largest pegmatite, GLF, attains 400 × 15 m.

Most of the pegmatites show a regular pattern of concentric zoning. The thin but continuous border zone consists of medium-grained oligoclase with microcline-perthite and quartz. Large crystals of graphic microcline-perthite + quartz intergrowths, embedded in coarse-grained albite + quartz ± biotite ± muscovite, constitute an extensive wall zone. The core consists of blocky microcline-perthite and quartz, occasionally segregated into a blocky core-margin of microcline-perthite surrounding a lenticular quartz core; cleavelandite and muscovite are widespread but subordinate. Layers and pods of fine- to medium-grained albite with quartz, muscovite, and garnet are located at the outer margins of the blocky core (or within and around the segregated microcline-perthite core margin), extensively replacing microcline-perthite and quartz. Most of the rare-element-bearing and other accessory minerals are concentrated in this unit. Garnet, beryl, and cordierite are associated with subordinate but widespread Nb-, Ta-, Ti-, and Sn-bearing oxide minerals, local monazite, gahnite, zircon, xenotime, and extremely rare apatite, pyrite, and chalcopyrite.

Despite the rather simple mineral assemblage and uniform internal structure, the Greer Lake pegmatites are conspicuously

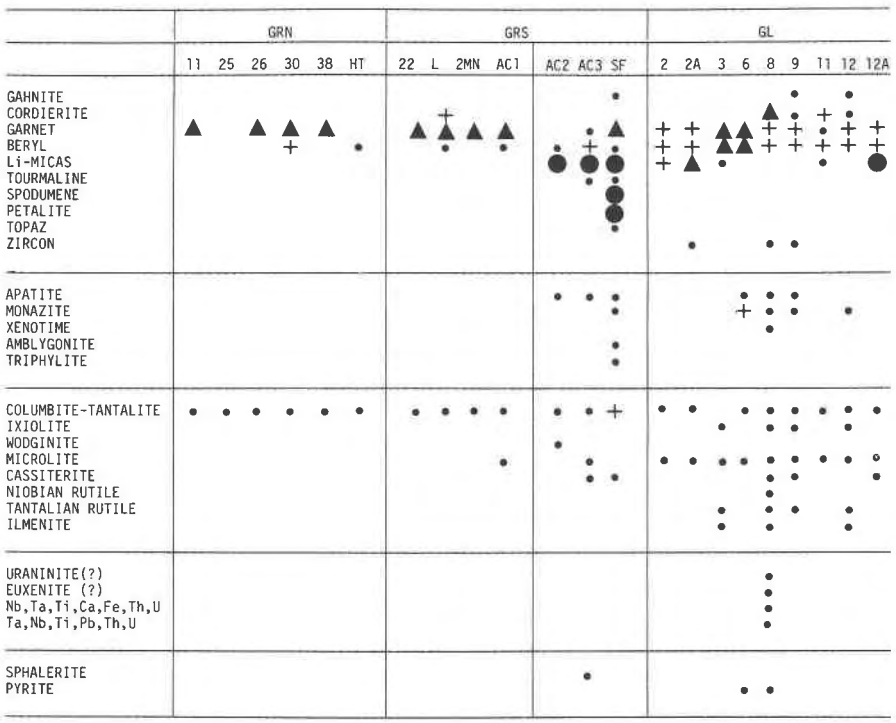

Fig. 3. Assemblages of Nb- and Ta-bearing oxide minerals and other subordinate and accesory phases at Greer Lake. Microcline-perthite, albite, quartz, and muscovite present at all locations. GRN = northern segment and GRS = southern segment of the Greer Lake granite; GL = Greer Lake pegmatites (see text for further details). ● = subordinate rock-forming constituent; ▲ = abundant accessory phase; + = subordinate accessory phase; • = rare mineral.

diversified. They range from bodies with predominant REE, Ti, Fe > Mn and Nb > Ta in their accessory minerals (GL6, GL8, GL9) to veins poor in Ti and REE but with Nb ≤ Ta, Fe ≤ Mn and increased Li and Cs in beryl (GL2, GL2A, GL11, GL12A). Variation in the accessory mineral assemblages coincides with a broad range of trace-element concentrations shown by the rock-forming minerals. For example, blocky microcline-perthite varies from 96 to 13 in K/Rb and from 10 to 1790 ppm of Cs; core-margin muscovite and late lithian micas range from 21.8 to 3.6 in K/Rb, from 1027 to 321 in K/Cs, and from 0.07 to 1.10 wt% of Li.

The internal structure, mineralogy, and geochemistry of the Greer Lake pegmatites indicate that they can be classified as partly albitized blocky microcline + muscovite dikes of the beryl-columbite type (Černý, 1982).

Nb- and Ta-bearing parageneses

The Nb- and Ta-bearing accessory minerals occur principally in four environments: (1) GRN—the potassic pegmatite phase of the main, northern, geochemically primitive part of the Greer Lake pegmatitic granite; (2) GRS—the potassic pegmatite phase of the southeastern, more fractionated segment of this granite, within the fault-bound greenstone wedge; (3) AC2, AC3, SF—the highly fractionated pegmatite pods within, and adjacent to GRS: the Annie Claim no. 2 and no. 3 and the Silverleaf offshoot; and (4) GL—the Greer Lake pegmatite group south of the southern fault. Figure 3 lists the associations of accessory minerals from all locations where Nb- and Ta-bearing minerals have been found.

Descriptive mineralogy

Experimental methods

All chemical analyses were done with a MAC 5 electron microprobe operating predominantly in wavelength-dispersive (WD) and partly in energy-dispersive (ED) modes. Standards used were cassiterite (Sn$L\alpha$), chromite (Fe$K\alpha$), titanite (Ti$K\alpha$), manganotantalite (Mn$K\alpha$, Ta$L\alpha$, $M\alpha$), stibiotantalite (Sb, Bi), pyrope (Al), Sc metal, $Ba_2NaNb_5O_{15}$, and $CaNb_2O_6$ (Nb$L\alpha$). Conditions of analysis were accelerating potentials of 20 and 15 kV, sample currents of 40 nA (WD) and 5 nA (ED) measured on brass (WD) and ZnS (ED), count times of 10 s (WD) and 200 s (live time; ED). Wavelength-dispersive spectral data were reduced by a locally modified version of the program EMPADR VII (Rucklidge and Gasparrini, 1969). Energy-dispersive spectra were collected with a KEVEX Model 7000 ED spectrometer and were reduced with KEVEX software utilizing the program MAGIC V (Colby, 1980). Peak-overlap problems encountered during analysis of ED spectra were resolved by stripping techniques involving library spectra. Compositions of ixiolite and niobian-tantalian rutile calculated with all iron as Fe^{2+} showed cations in excess of structurally available sites. Recalculation of unit-cell contents was adjusted by converting as much Fe to Fe^{3+} as required to eliminate the cation surplus. The crystallochemical assumptions of Ercit (1986) were applied to the calculation of unit-cell contents of both AC2 wodginites.

Electron-microprobe analyses of microlite were obtained under the same ED instrumental conditions as for columbite-tantalite, and with the same standards for Ti, Sn, Fe, Mn, and Nb. Other

Table 1. Chemical composition of columbite-tantalites from Greer Lake pegmatitic granite

Sample number	Ta_2O_5	Nb_2O_5	TiO_2	SnO_2	Al_2O_3	Sb_2O_3	MnO	FeO	CaO	Total
GRHT	15.5	63.0	0.4	0.05	-	0.1	7.8	12.2	0.06	99.11
GR30A1	20.7	59.2	0.8	-	0.03	-	2.3	16.6	0.05	99.68
GR2MNA	40.8	41.7	0.3	0.4	-	-	7.8	10.1	-	101.1
GR22A2	51.0	32.0	0.3	0.3	-	-	5.4	11.5	-	100.5
SF22	37.9	40.8	0.2	4.6	-	-	15.4	1.5	-	100.4
SFTM	62.9	20.4	0.02	0.7	-	-	15.6	0.05	0.3	99.97
AC1AL	57.2	23.9	0.9	0.5	-	0.1	4.7	11.2	0.04	98.54
AC31D	67.6	15.9	0.2	0.1	-	-	13.1	1.9	0.04	98.94*
AC32B	77.5	7.8	0.1	0.4	-	-	14.2	0.2	-	100.2
	Ta^{5+}	Nb^{5+}	Ti^{4+}	Sn^{4+}	Al^{3+}	Sb^{3+}	Mn^{2+}	Fe^{2+}	Ca^{2+}	Total
GRHT	1.02	6.88	0.07	0.005	-	0.01	1.60	2.47	0.02	12.075
GR30A1	1.38	6.55	0.15	0.01	0.01	-	0.48	3.40	0.01	11.99
GR2MNA	2.94	4.99	0.06	0.04	-	-	1.75	2.24	-	12.02
GR22A2	3.88	4.05	0.06	0.03	-	-	1.28	2.69	-	11.99
SF22	2.74	4.91	0.04	0.49	-	-	3.47	0.33	-	11.98
SFTM	5.13	2.77	0.005	0.08	-	-	3.97	0.01	0.10	12.065
AC1AL	4.60	3.20	0.20	0.06	-	0.01	1.18	2.77	0.01	12.03
AC31D	5.72	2.24	0.05	0.01	-	-	3.45	0.49	0.01	12.02**
AC32B	6.82	1.14	0.02	0.05	-	-	3.93	0.05	-	12.01
Natural		a, Å			b, Å			c, Å		V, Å^3
GR30A1		14.230(10)			5.725(4)			5.081(5)		413.9(7)
GR2MNA		14.275(6)			5.728(2)			5.085(2)		415.8(5)
GR22A2		14.248(8)			5.721(3)			5.092(3)		415.1(6)
SF22		14.277(4)			5.748(2)			5.150(3)		422.7(2)
AC32B		14.402(3)			5.751(1)			5.102(1)		422.6(2)
Heated										
GR30A1		14.280(9)			5.736(3)			5.053(4)		413.9(5)
GR2MNA		14.339(5)			5.738(2)			5.058(3)		416.2(3)
SF22		14.417(4)			5.756(2)			5.084(2)		421.9(2)
AC32B		14.411(2)			5.755(1)			5.085(1)		421.7(1)

Unit cell contents and unit cell dimensions calculated for the ordered cell (24 oxygens); - not detected; * includes 0.1 wt.% MgO; ** includes 0.05 Mg. Numerals in brackets represent $\pm 1\sigma$ in terms of the last decimal place.

Table 2. Chemical composition of columbite-tantalites from Greer Lake pegmatites

Sample number	Ta_2O_5	Nb_2O_5	TiO_2	SnO_2	Sc_2O_3	MnO	FeO	CaO	Total
GL2A-18	64.0	17.2	2.3	0.7	-	11.0	4.0	-	99.2
GL6-1	17.7	56.4	3.1	2.4	1.4	8.1	9.2	0.06	98.36
GL8C-31-6	26.6	47.1	4.6	-	1.5	6.0	9.7	0.3	96.0*
GL8W-1	27.8	48.3	3.8	1.3	0.7	6.8	9.9	-	98.0
GL9-18-3	39.5	37.7	4.7	0.6	1.3	8.2	8.8	-	100.8
GL9-19	51.0	25.2	5.2	2.5	0.8	7.8	7.1	-	99.6
GL12-1	34.6	43.5	3.6	0.8	0.6	9.5	8.0	-	100.6
GL12A-1	72.2	11.4	1.2	1.6	-	13.4	1.2	-	101.0
	Ta^{5+}	Nb^{5+}	Ti^{4+}	Sn^{4+}	Sc^{3+}	Mn^{2+}	Fe^{2+}	Ca^{2+}	Total
GL2A-18	5.25	2.34	0.51	0.08	-	2.81	1.01	-	12.00
GL6-1	1.17	6.19	0.57	0.23	0.30	1.67	1.87	0.02	12.02
GL8C-31-6	1.85	5.45	0.89	-	0.33	1.30	2.08	0.08	11.99**
GL8W-1	1.91	5.51	0.72	0.13	0.15	1.45	2.09	-	11.96
GL9-18-3	2.77	4.40	0.91	0.06	0.29	1.79	1.90	-	12.12
GL9-19	3.83	3.18	1.08	0.28	0.19	1.83	1.64	-	12.03
GL12-1	2.40	5.01	0.69	0.08	0.13	1.73	2.02	-	12.06
GL12A-1	6.09	1.60	0.28	0.20	-	3.52	0.31	-	12.00
Natural		a, Å			b, Å			c, Å		V, Å^3
GL2A-18		14.247(10)			5.739(3)			5.147(7)		420.8(4)
GL6-1		14.186(5)			5.721(3)			5.128(2)		416.2(2)
GL8C-31-6		14.173(6)			5.709(3)			5.108(2)		413.3(3)
GL9-19		14.177(3)			5.716(1)			5.114(2)		414.4(1)
GL12-1		14.217(6)			5.722(3)			5.144(2)		418.5(3)
GL12A-1		14.247(3)			5.741(2)			5.151(2)		421.3(2)
Heated										
GL2A-18		14.349(4)			5.742(2)			5.083(2)		418.8(2)
GL8C-31-6		14.299(4)			5.732(1)			5.064(2)		415.1(2)
GL9-19		14.271(6)			5.724(2)			5.063(2)		413.6(3)
GL12-1		14.320(5)			5.732(2)			5.074(3)		416.5(3)
GL12A-1		14.380(4)			5.746(1)			5.084(2)		420.1(2)

Unit cell contents and unit cell dimensions calculated for the ordered cell (24 oxygens); - not detected; * includes 0.2 wt.% UO_2; ** includes 0.01 U. Numerals in brackets represent $\pm 1\sigma$ in terms of the last decimal place.

standards for microlite were uranium (U), microlite (Na, Ca, Ta), ThO_2 (Th), and PbTe (Pb). Peak-stripping techniques were used to resolve overlap problems, using library spectra derived from spectra of microprobe standards with matrices similar to the sample. Noniterative stripping was used in cases of minor overlap. More severe overlap problems (e.g., Nb-Pb and U-Sn-Ca) were dealt with by deconvoluting the region of interest prior to energy stripping, using simple iterative methods and the same library spectra used in the noniterative approach. Unit-cell contents were calculated assuming ΣB-site = 4, and all Sn as Sn^{2+} unless ΣA-site exceeded 4. In such a case both ΣA and ΣB were adjusted to 4 by converting an adequate part of Sn^{2+} to Sn^{4+}, giving a minimum theoretical estimate of Sn^{4+}/Sn^{2+}.

Unit-cell dimensions were calculated from X-ray powder-diffraction data obtained with Philips X-ray diffractometers using Ni-filtered or graphite-monochromated Cu$K\alpha$ radiation (λ = 1.5418 Å) and scanning speeds of 0.25° to 0.5° 2θ/min. A minimum of 8 and a maximum of 22 reflections measured between 10° and 70° 2θ were used in least-squares refinement of the data. Annealed CaF_2 (a = 5.4620 Å) was used as an internal calibration standard. A modified version of the program CELREF (Appleman and Evans, 1973) was used for unit-cell refinement.

In the heating experiments, separate fragments 0.5 to 2 mm in size were heated in air at 1000°C for 16 h. Heating relatively coarse grained material minimizes oxidation of Fe^{2+} to such a degree that unit-cell dimensions of columbite-tantalites heated in air and in a controlled atmosphere (CO/CO_2 = 2.5/1) are statistically identical (unpub. data of P. Černý and A. C. Turnock).

Columbite-tantalite

Minerals of the columbite-tantalite group are the most abundant and widespread Nb- and Ta-bearing phases in this granite pegmatite suite. Small lath-shaped crystals are typical of the GRN and GRS occurrences, whereas large anhedral grains (to 2 cm) and subhedral crystals (to 8 cm) are found in AC and SF. Lath-shaped crystals occur locally in the GL pegmatites, but microgranular aggregates intimately associated with other Nb-, Ta-, Ti-, and Sn-bearing minerals are much more common.

Representative compositions of columbite-tantalite indicate that the GRN, GRS, AC, and SF minerals are poor in Ti and, with the exception of SF, also in Sn (Tables 1 and 2, Fig. 4). In contrast, many of the GL columbite-tantalites are distinctly enriched in both Sn and Ti (Fig. 5, Table 2), and they grade into the compositions typical of ixiolite.

The structural state of columbite-tantalites can be represented on an a-c diagram shown in Figure 6 (Černý and Turnock, 1971; cf. Wise et al., 1985, and Černý and Ercit, 1985, for end-member data). The cell dimensions are sensitive to both the Fe/Mn substitution (primarily affecting a) and the order-disorder (affecting a and c alike). The order-disorder vector is parallel to the lines connecting equal end-member compositions.

The columbite-tantalites show widely variable degrees

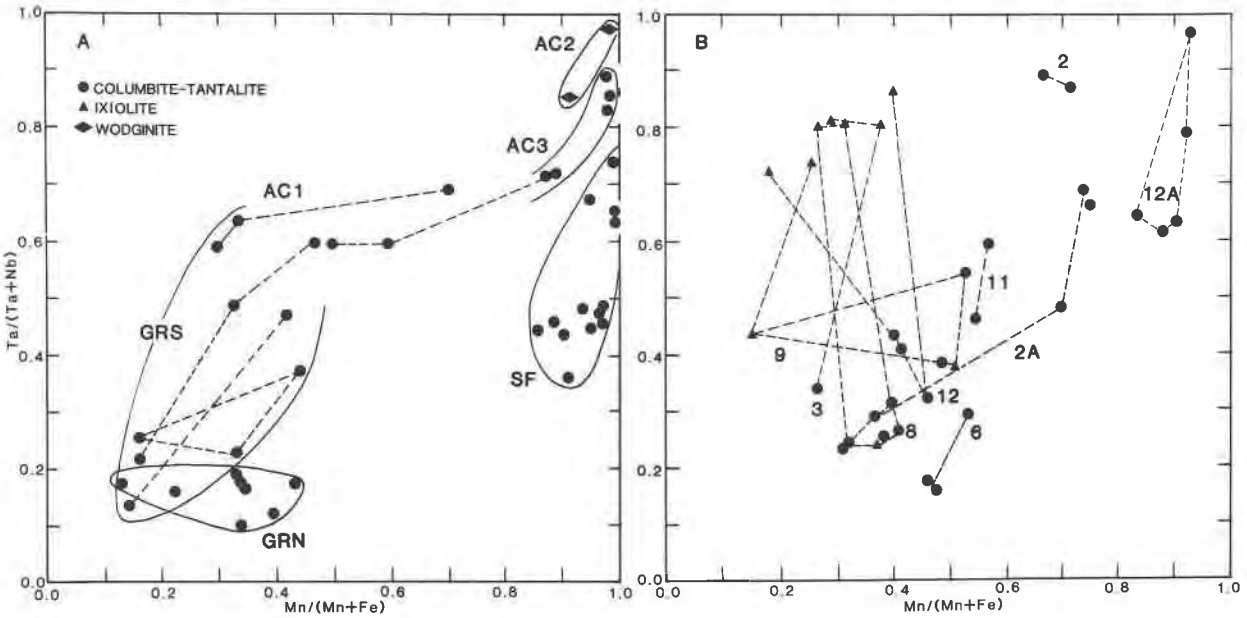

Fig. 4. Compositions of the Greer Lake Fe-, Mn-, Nb-, and Ta-bearing oxide minerals in the columbite-tantalite-tapiolite quadrilateral. (A) Occurrences in the pegmatitic granite; (B) minerals from the pegmatite veins. Atomic ratios with all Fe as Fe^{2+}.

of order-disorder, but they cluster into well-defined groups according to their provenance; (1) both GRN and GRS minerals show intermediate structural states; (2) the AC and SF samples show moderate and extensive variation, respectively; the AC data indicate intermediate to considerably ordered structures, the SF minerals have nearly disordered to considerably ordered structures; (3) the GL columbite-tantalites are highly to totally disordered, corresponding to "pseudo-ixiolite" of Nickel et al. (1963).

On heating, the columbite-tantalites develop ordered structures that plot close to the joins of fully ordered synthetic end members of the *a-c* diagram. These data are not included in Figure 6 to avoid cluttering, but examples of the GL data are shown in Černý and Turnock (1971).

Ixiolite

Ixiolite is restricted to the GL pegmatites and always occurs in fine-grained (<0.5 mm) aggregates of diverse

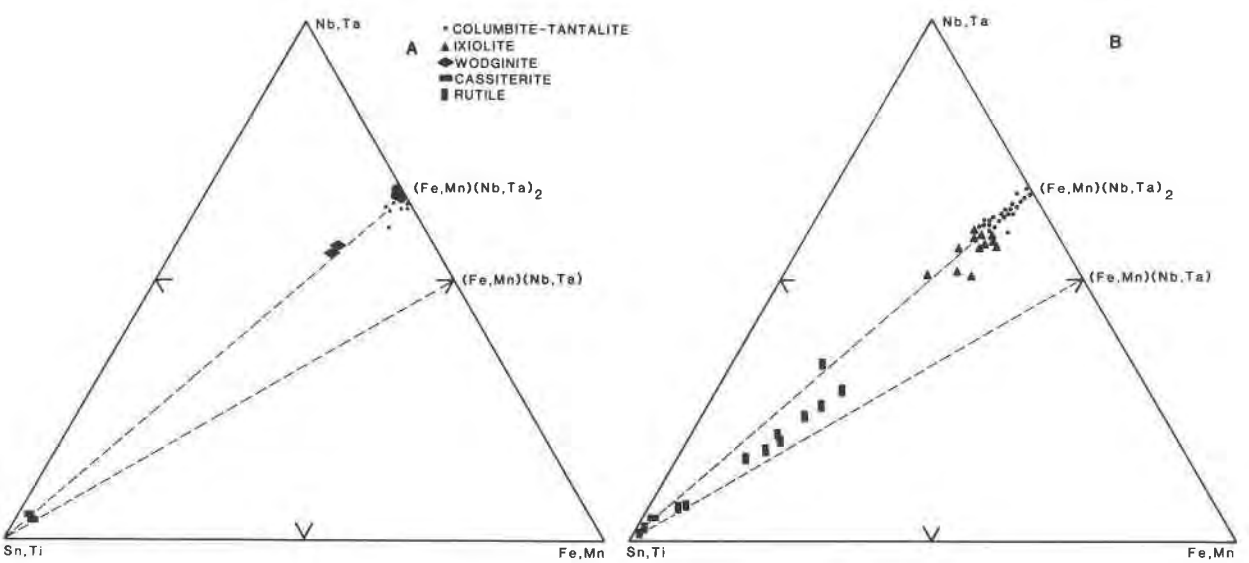

Fig. 5. Composition of the Greer Lake Nb- and Ta-bearing oxide minerals in the (Sn,Ti)-(Nb,Ta)-(Fe,Mn) diagram. (A) Occurrences in the pegmatitic granite; (B) minerals from the pegmatite veins. Black field in A is populated by 32 columbite-tantalites. Atomic ratios with all Fe as Fe^{2+}.

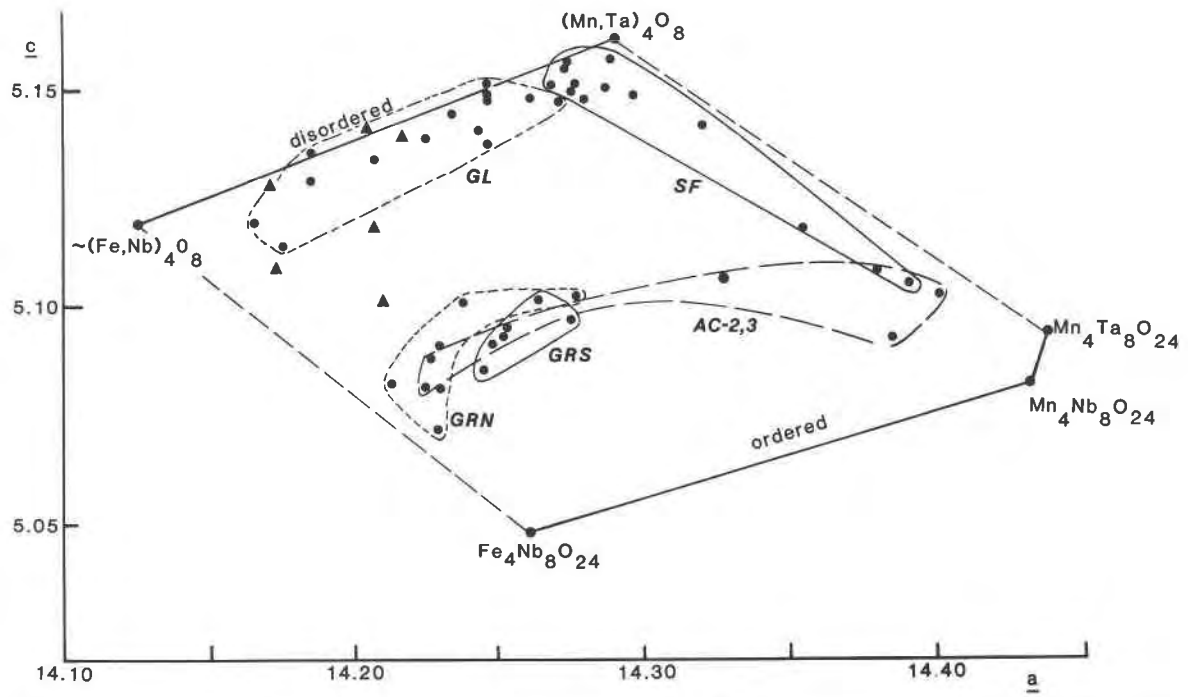

Fig. 6. The *a-c* diagram of structural order-disorder for the Greer Lake columbites-tantalites. Ixiolites (triangles) from the GL pegmatites are shown for comparison. All data for *a* relate to the ordered unit-cell dimension, irrespective of the actual degree of disorder. See text for sources of the end-member values.

Nb-, Ta-, Ti-, and Sn-bearing oxide minerals. It is commonly associated with niobian and tantalian rutile, ilmenite, and cassiterite; however, it is rare in Nb-, Ta-, Ti-, and Sn-bearing nodules containing Sn- and Ti-poor columbite-tantalite, and the two minerals do not occur in mutual contact.

The ixiolites have distinctly higher Ta/(Ta + Nb) ratios than columbite-tantalites of corresponding Mn/(Mn + Fe) ratio, and they typically plot within the two-phase tantalite + tapiolite region of the quadrilateral (Table 3, Figs. 4B, 5B; cf. Fig. 1 of Černý and Ercit, 1985). In Figure 5B, the GL ixiolites generally plot along the (Sn,Ti)-(Fe,Mn)(Nb,Ta)$_2$ join, extending from the columbite-tantalite data. This indicates the dominance of the substitution (Fe,Mn) + 2(Nb,Ta) ⇌ 3(Sn,Ti), which reaches much higher levels here than in stannian-titanian columbite-tantalite. Most of the deviations plot between the (Sn,Ti)-(Fe,Mn)(Nb,Ta)$_2$ and (Sn,Ti)-(Fe,Mn)(Nb,Ta) joins, and their cation totals normalized to 24 oxygens exceed 12.00. Both these features suggest the presence of Fe^{3+}, which seems to be typical of ixiolite in general (e.g., Borisenko et al., 1969). Calculated values of Fe^{3+} are shown in Table 3. Ixiolite GL8C31-3, the most enriched in R^{4+} (25.1 at.% Sn + Ti), has cation ratios close to those of ideal wodginite ($R^{2+}_4R^{4+}_4R^{5}_8O_{32}$). This represents the maximum level attained by the above substitution in columbite-wodginite-ixiolite structures.

It is noteworthy that most of the GL ixiolites are Ti-rich with only subordinate Sn. Stannian ixiolites are generally much more common (Khvostova et al., 1983; Černý and Ercit, 1985). Scandium is another element that locally enters ixiolite in substantial amounts (v. Knorring et al., 1969; Borisenko et al., 1969) but does not accumulate in columbite-tantalite. Surprisingly, the subordinate Sc contents in the orthorhombic GL phases are, on average, high

Table 3. Chemical composition of ixiolites from Greer Lake pegmatites

Sample number	Ta_2O_5	Nb_2O_5	TiO_2	SnO_2	Sc_2O_3	Fe_2O_3	FeO	MnO	Total
GL3-15-2	66.6	9.7	3.1	4.6	-	2.5	6.9	5.4	98.8
GL3-15-8	66.6	9.3	3.5	5.2	-	0.7	9.1	3.9	98.3
GL8C-31-3	20.9	39.7	4.0	19.5	1.1	0.2	8.4	5.0	98.8
GL8C-32-13	66.5	9.9	3.4	4.3	-	3.3	8.1	3.9	99.3
GL8C-32-24	65.3	9.3	3.0	4.7	-	4.1	6.6	4.6	97.6
GL-18-5	59.0	12.5	8.0	4.5	0.5	4.5	6.9	3.7	99.7
GL9-18-2	41.9	32.4	6.0	1.8	0.8	4.2	10.7	2.5	100.3
GL9-18	36.8	35.8	8.6	3.2	0.6	0.3	7.3	7.8	100.4
GL12-1-5	57.0	12.8	7.1	4.9	0.1	7.3	6.6	2.8	98.5
GL12-1-4	68.5	6.4	2.8	6.6	-	3.1	5.8	5.6	98.8
	Ta^{5+}	Nb^{5+}	Ti^{4+}	Sn^{4+}	Sc^{3+}	Fe^{3+}	Fe^{2+}	Mn^{2+}	Total
GL3-15-2	5.60	1.36	0.72	0.57	-	0.58	1.77	1.41	12.00
GL3-15-8	5.65	1.31	0.82	0.65	-	0.16	2.37	1.03	12.00
GL8C-31-3	1.46	4.60	0.77	1.99	0.25	0.05	1.80	1.09	12.00
GL8C-32-13	5.52	1.37	0.78	0.52	-	0.75	2.06	1.01	12.00
GL8C-32-24	5.52	1.31	0.70	0.58	-	0.95	1.73	1.21	12.00
GL9-18-5	4.55	1.60	1.71	0.51	0.12	0.97	1.64	0.89	12.00
GL9-18-2	2.96	3.80	1.17	0.19	0.18	0.82	2.33	0.55	12.00
GL9-18	2.53	4.10	1.64	0.32	0.13	0.07	1.54	1.67	12.00
GL12-1-5	4.43	1.65	1.53	0.56	0.03	1.56	1.57	0.68	12.00
GL12-1-4	5.85	0.91	0.66	0.83	-	0.74	1.52	1.49	12.00
Natural	a, Å		b, Å		c, Å		V, Å^3		
GL3-15-2	14.206(3)		5.729(1)		5.141(1)		418.4(1)		
GL8C-31-13	14.208(3)		5.722(1)		5.118(1)		416.1(1)		
GL9-18-2	14.172(8)		5.719(3)		5.127(3)		415.5(4)		
GL12-1-4	14.136(12)		5.737(3)		5.157(12)		418.2(7)		

Unit cell contents (based on 8 oxygens) tripled for ease of comparison with columbite-tantalites in Tables 1 and 2; - not detected. Numerals in brackets represent ±1σ in terms of the last decimal place.

Table 4. Chemical composition of wodginites, niobian and tantalian rutiles, cassiterites, and ilmenite from Greer Lake pegmatitic granite and pegmatites

Mineral	Sample number	Ta_2O_5	Nb_2O_5	TiO_2	SnO_2	Fe_2O_3	FeO	MnO	Total
W	AC2-81-IV	70.9	1.2	-	14.4	0.2	0.0	11.2	97.9[1]
W	AC2-79	64.6	6.6	0.2	15.8	1.1	0.0	10.7	99.2[1]
R	GL3-15-9	34.8	8.3	43.2	2.2	8.2	4.2	-	100.9
R	GL8C-32-12	7.6	4.9	82.4	1.8	4.1	0.7	-	101.5
R	GL8W-28	18.4	15.9	52.4	2.5	8.0	3.7	-	100.9[3]
R	GL9-18	44.9	6.0	34.2	1.5	8.4	5.0	-	100.2[3]
C	SF14	4.7	-	-	94.4	-	0.7	0.2	100.0
C	SF15	4.9	-	-	94.0	-	1.0	0.05	99.95
C	GL8C-31-4	3.3	1.3	-	93.0	-	0.9	-	98.5
IL	GL8W-28	0.8	0.2	51.0	-	-	35.7	11.0	98.7

		Ta^{5+}	Nb^{5+}	Ti^{4+}	Sn^{4+}	Fe^{3+}	Fe^{2+}	Mn^{2+}	Total
W	AC2-81-IV	8.72	0.25	-	2.60	0.07	0.00	4.29	15.93[2]
W	AC2-79	7.52	1.28	0.06	2.70	0.35	0.00	3.88	15.88[2]
R	GL3-15-9	0.34	0.13	1.16	0.03	0.22	0.13	-	2.00
R	GL8C-32-12	0.06	0.06	1.75	0.02	0.09	0.02	-	2.00
R	GL8W-28	0.16	0.23	1.28	0.03	0.20	0.10	-	2.00
R	GL9-18	0.47	0.10	0.99	0.02	0.24	0.16	-	2.00[4]
C	SF14	0.07	-	-	1.90	-	0.03	0.01	2.01
C	SF15	0.07	-	-	1.89	-	0.04	0.002	2.002
C	GL8C-31-4	0.05	0.03	-	1.89	-	0.04	-	2.01
IL	GL8W-28	0.03	0.02	5.91	-	-	4.61	1.44	12.01

	Natural	a, Å	b, Å	c, Å	β, °	V, Å^3
W	AC2-79	9.523(3)	11.476(3)	5.142(2)	90.78(3)	561.9(2)
R	GL8W-28	4.634(1)	-	3.001(2)	-	64.4(1)
R	GL9-18	4.651(1)	-	3.004(1)	-	65.0(1)
C	SF15	4.734(1)	-	3.184(1)	-	71.4(1)
	Heated					
W	AC2-79	9.527(2)	11.471(3)	5.119(1)	91.15(2)	559.2(1)
R	GL8W-28	4.632(2)	-	2.999(4)	-	64.3(2)
R	GL9-18	4.645(1)	-	3.001(1)	-	64.7(1)
C	SF15	4.735(1)	-	3.179(1)	-	71.3(1)

Unit cell contents based on 32 oxygens for wodginite (W), on 4 oxygens for rutile (R) and cassiterite (C), and on 18 oxygens for ilmenite (IL); - not detected; [1]total includes 0.2 CaO; [2]total includes 0.09 Ca^{2+}; [3]total includes 0.2 Sc_2O_3; [4]total includes 0.01 Sc^{3+}. Numerals in brackets represent $\pm 1\sigma$ in terms of the last decimal place.

in columbite-tantalites relative to the ixiolites. In contrast, Sc is not detectable in the GRN, GRS, AC, and SF columbite-tantalites.

The ixiolites produce X-ray diffraction patterns typical of disordered columbite-tantalite. Table 3 and Figure 6 show the unit-cell dimensions of ixiolite with *a* tripled, for easy comparison with columbite-tantalites in Tables 1 and 2 and in Figure 6. On heating, the ixiolites adopt the wodginite structure (cf. Černý and Ercit, 1985). Cell dimensions of the heating products of GL ixiolites could not be adequately refined because of peak overlap with admixed phases. Nevertheless, the diffractions typical of wodginite were unequivocally identified in the powder patterns in all samples listed in Table 3.

The heating products of some of the "columbite-tantalites" containing 8–11 at.% ΣR^{4+} (Fig. 5B) could not be unambiguously identified, because of the presence of additional phases and the uncertain nature of some of their prominent diffractions. Thus it is possible that some of these samples convert to (weakly monoclinic) wodginite, completely or in part. Komkov (1970) stated that a wodginite component develops, along with an ordered columbite-tantalite phase, in amounts proportional to the (Sn,Ti) content of the natural disordered minerals. We could not observe such a relationship in our current studies (unpub. data of P. Černý and M. A. Wise); however, this discrepancy may be due only to delicate differences in the heating and cooling procedures. In any case, Komkov's (1970) results and the continuous gradation from the rather pure GL columbite-tantalites into typical R^{4+}-rich ixiolites cast doubt on the existence of a sharp, quantitatively definable boundary between columbite-tantalite and ixiolite.

Wodginite

Wodginite occurs only at the AC2 locality, where two large subhedral grains (2 and 4 cm across) associated with cleavelandite were found along the contact of blocky microcline-perthite with quartz. The sample AC2-79 has a composition close to that of ideal wodginite (Table 4) but with some vacancies and extensive Ta substitution for Sn at the C site. Cell dimensions are appreciably monoclinic, enhanced by heating to a β angle close to its highest known value for natural and/or heated wodginites (Ercit et al., 1984). In contrast, the AC2-81-IV specimen shows broad diffraction peaks corresponding to tantalite. The Mn content of AC2-81-IV exceeds that allowed by wodginite stoichiometry. The sample may represent a submicroscopic intergrowth of manganotantalite and wodginite, and it deserves detailed examination by electron microscopy and diffraction.

Niobian and tantalian rutile

These varieties of rutile occur exclusively in the GL pegmatites, mostly as microscopic grains associated with other Nb-, Ta-, Ti-, and Sn-bearing minerals. They are particularly common in close association and intimate intergrowth with ixiolite and ilmenite.

At other localities, niobian and tantalian rutiles commonly form primary subhedral to euhedral crystals (the niobium-rich varieties usually bearing exsolved titanian ixiolite), or they occur as exsolution blebs in primary crystals of titanian ixiolite. In the GL samples, both niobian and tantalian rutile occur as anhedral grains coexisting with other Nb- and Ta-bearing phases, with no indication of exsolution or metasomatic relationship.

Rutile compositions vary widely in $Ti/(R^{2+} + R^{5+})$ and Ta/(Ta + Nb) but always show extremely high Fe/(Fe + Mn) (Table 4, Fig. 5B). Cation totals calculated with ΣFe as Fe^{2+} exceed the theoretical maximum of 2.00 per unit cell, suggesting the presence of Fe^{3+}. This is also indicated by the location of most of the rutile compositions between the (Sn,Ti)-$(Fe,Mn)(Nb,Ta)_2$ and (Sn,Ti)-(Fe,Mn)(Nb,Ta) joins of Figure 5B. Table 4 shows unit-cell contents calculated for a Fe^{2+}/Fe^{3+} ratio yielding $\Sigma cat. = 2$. All these characteristics are in agreement with the general behavior of niobian-tantalian rutiles from other localities (Černý et al., 1981b; Foord, 1982; Černý and Ercit, 1985).

Cassiterite

Cassiterite is not common at Greer Lake. It occurs in significant quantities only in the most fractionated pegmatite pods (AC3 and SF) of the southwestern segment of the pegmatitic granite and as very rare microscopic grains in some of the GL pegmatites. It is rather poor in

Table 5. Chemical composition of microlites from Greer Lake pegmatitic granite and pegmatites

Sample number	Ta_2O_5	Nb_2O_5	TiO_2	CaO	Na_2O	SnO_2	SnO	UO_2	FeO	MnO	Total	
AC1-B	78.6	0.3	0.4	9.5	2.1	-	1.2	-	0.2	0.05	92.45*	
GL3-15-4	64.9	10.3	2.7	12.6	3.5	-	2.0	-	0.4	-	96.4	
GL8C-32-7	52.2	14.7	7.6	8.3	1.6	-	-	6.7	2.2	-	93.3	
GL9-18	74.4	2.4	1.5	12.3	4.3	0.2	0.7	0.1	0.8	-	96.6	
GL12-1-3	74.0	2.8	1.8	12.8	4.3	1.0	0.7	0.1	0.5	0.4	98.4	
GL12A-2-4	78.3	1.0	0.4	10.8	4.0	-	0.1	0.3	0.3	0.05	95.25	
	Ta^{5+}	Nb^{5+}	Ti^{4+}	Ca^{2+}	Na^{+}	Sn^{4+}	Sn^{2+}	U^{4+}	Fe^{2+}	Mn^{2+}	Total	Eff.O
AC1-B	3.92	0.03	0.06	1.87	0.75	-	0.10	-	0.03	0.01	2.78**	12.36
GL3-15-4	2.90	0.77	0.33	2.22	1.12	-	0.15	-	0.06	-	3.55	12.81
GL8C-32-7	2.14	1.00	0.86	1.34	0.47	-	-	0.22	0.28	-	2.31	11.87
GL9-15	3.60	0.19	0.20	2.34	1.48	0.01	0.05	0.005	0.12	-	3.985	13.16
GL12-1-3	3.48	0.22	0.23	2.37	1.44	0.07	0.05	0.005	0.07	0.06	4.135	13.13
GL12A-2-4	3.86	0.08	0.06	2.10	1.41	-	0.01	0.01	0.05	0.01	3.58	12.86

Contents of 0.25 unit cell normalized to ΣB cations (Ta+Nb+Ti) = 4.00; - not detected.
Totals of 0.25 unit cell contents give ΣA cations ($Ca+Na+Sn^{2+}+U^{4+}+Fe+Mn+Sb^{3+}$).
* includes 0.1 Sb_2O_3
**includes 0.01 Sb^{3+}

the "tapiolite" component, but it shows the same strong Ta > Nb and Fe > Mn preferences as rutile (Table 4).

Microlite

Microlite is absent from the GRN localities but occurs in minor quantities in AC1 and AC3 locations of GRS. It is also found as microscopic grains in fine-grained aggregates of Nb-, Ta-, Ti-, and Sn-bearing minerals in all GL pegmatites. Microlite forms rounded grains coexisting with columbite-tantalite or ixiolite, or veins and metasomatic patches penetrating these minerals.

Microlite compositions are highly variable in all respects. Table 5 shows representative examples of compositions that gave realistic totals (with allowance for H_2O and F_2) and acceptable formulae when normalized to ΣB-site = 4 (cf. Experimental Methods and Ercit et al., 1985). Many microlite grains are altered, being inhomogeneous in reflected light and giving electron-microprobe totals of 78 to 85 wt%. This is particularly typical of microlites enriched in U (to 8.7 wt% UO_2) and Bi (to 27 wt% Bi_2O_3). None of the Bi-bearing microlites conforms to a realistic microlite stoichiometry.

Ilmenite

Ilmenite occurs in several of the GL pegmatites as rare microscopic grains or skeletal aggregates intimately intergrown with niobian-tantalian rutile or associated with ixiolite. Only a single electron-microprobe analysis gave acceptable stoichiometry, with very low (Nb,Ta) but surprisingly high Mn (Table 4); beam overlap with adjacent phases was the most probable cause of appreciable deviations in other data. The slight deviation from the $A_6B_6O_{18}$ formula in favor of the A sites (i.e., Fe,Mn) suggests a limited quantity of hematite in solid solution.

Unidentified phases

Several unidentified phases were repeatedly analyzed, but their nature could not be determined. These minerals are invariably somewhat heterogeneous on the scale of the optical microscope; they are U and Th bearing and probably metamict as the totals of their chemical analyses vary between 74 and 85 wt%. Two compositions are encountered most frequently. One of them has substantial $Nb_2O_5 \gtrless Ta_2O_5$ (XO wt%), subordinate $ThO_2 > UO_2$ (2–4 wt%) and $TiO_2 >$ (CaO,FeO) (7–10 and 2–4 wt%, respectively). The other phase has $Ta_2O_5 > Nb_2O_5$ (XO wt%) and $PbO > ThO_2 > UO_2$ (1–8 wt% of each). A euxenite-like phase rich in Y is rather rare.

Element partitioning among Nb- and Ta-bearing phases

The distribution of elements among coexisting phases is indicative of their individual crystallochemical preferences and/or stabilities under given *P-T* conditions in the different bulk compositions of their parent system. In the mineral associations examined, the spectrum of elements involves some or all of Na, Ca, Fe^{2+}, Mn, Sn, Ti, Nb, Ta, O, and F. Other subordinate cations, such as Fe^{3+} and Sc, do not stabilize any of the mineral species present, but U, Th, and nonradiogenic Pb may have some control over the crystallization of the unknown phases. Thus it is desirable to review the compositional relationships among the coexisting phases. However, it should be emphasized that these are not necessarily equilibrium relationships. This is particularly relevant to the fine-grained aggregates from the GL pegmatites: their complex mineralogy, fine grain size, and the variable composition of different grains of the same species in a single aggregate all indicate rapid nucleation and growth, triggered by a sudden change in conditions of the parent fluid, and a lack of later re-equilibration.

Ixiolite and columbite-tantalite vs. niobian-tantalian rutile

With one prominent exception, columbite-tantalite and ixiolite are enriched in Nb and Mn with respect to coexisting niobian-tantalian rutile (Fig. 7A), in agreement with previous data (Černý et al., 1981b). However, nonequilibrium is indicated by the coexistence of a single orthorhombic phase with two different rutile compositions, and by an ixiolite + tantalian rutile pair with reversed Nb/Ta partitioning. Compositions of niobian-tan-

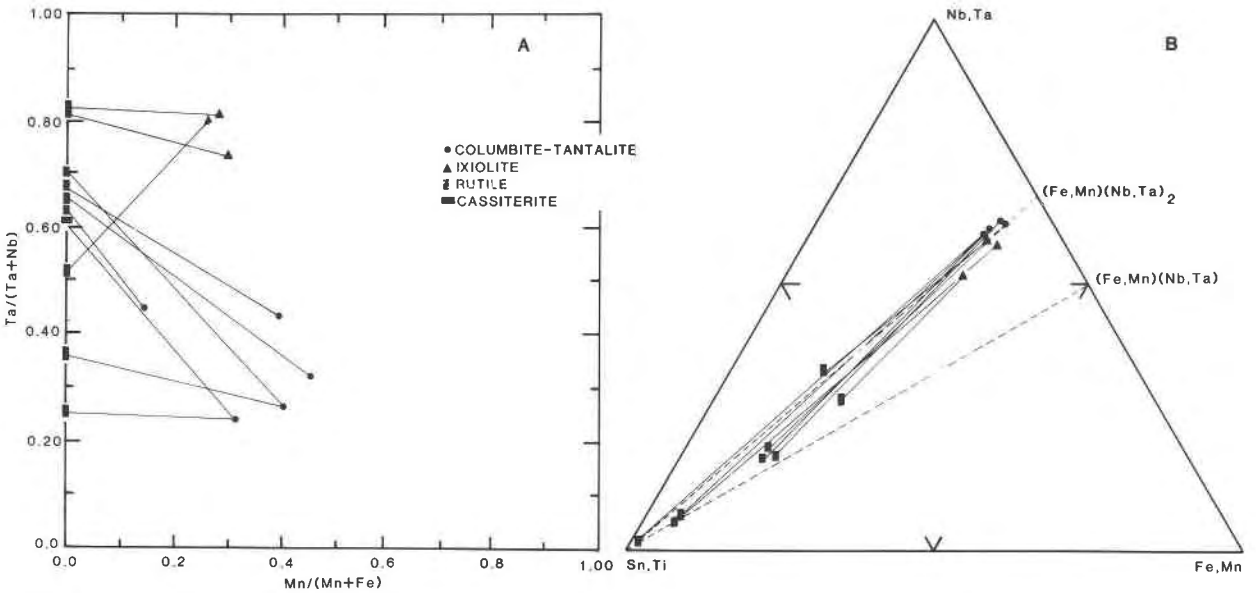

Fig. 7. Compositions of coexisting minerals (except microlite) in the columbite-tantalite-tapiolite quadrilateral, and in the (Sn,Ti)-(Nb,Ta)-(Fe,Mn) diagram. Atomic ratios with all Fe as Fe^{2+}.

talian rutiles and coexisting orthorhombic phases suggest a markedly asymmetric shape of the TiO_2-$(Fe,Mn)(Nb,Ta)_2O_6$ solvus, with a steep slope on the columbite-tantalite side (Fig. 7B). This is in agreement with other mineral pairs that may be closer to equilibrium (Černý et al., 1981b; Černý and Ercit, 1985).

Ixiolite and columbite-tantalite vs. cassiterite

The few data available indicate a strong preference of cassiterite for Ta and Fe relative to Nb and Mn, in agreement with the data of Wise and Černý (1984a) and Černý et al. (1985b).

Niobian-tantalian rutile vs. cassiterite

Both rutile and cassiterite concentrate Fe and Ta relative to Mn and Nb in the coexisting orthorhombic Fe-, Mn-, Nb-, and Ta-bearing minerals. The principal reasons are evidently those suggested by Weitzel (1976) to account for the difference in structure and symmetry between columbite-tantalite and tapiolite, namely the interrelationship between the difference in polarizing effects of Ta^{5+} and Nb^{5+} on one hand and between the ionic radii of Fe^{2+} and Mn^{2+} on the other. In contrast, the partitioning of Fe/Mn and Nb/Ta between rutile and cassiterite is virtually unknown, as this assemblage is extremely rare. A single coexisting rutile + cassiterite pair (GL8C-31) shows Ta/(Ta + Nb) higher in cassiterite than in rutile, a relationship suggested by the general compositional ranges of these minerals in separate pegmatite occurrences (Fig. 4 in Černý and Ercit, 1985) and observed for coexisting cassiterite + rutile from Tanco (T. S. Ercit, 1985, pers. comm.).

Niobian-tantalian rutile vs. ilmenite

This mineral pair should not be particularly scarce in granitic pegmatites, but there is little compositional data for coexisting pairs. The GL8W-28 ilmenite (Table 4) has negligible Σ(Ta,Nb) relative to rutile, with a possible preference of ilmenite for Ta relative to Nb. Ilmenite does concentrate Mn relative to the highly ferroan rutile composition. Another rutile + ilmenite pair from the GL8C-32 specimen shows the same Fe/Mn partitioning but about equal Nb/Ta in both minerals.

Ixiolite, columbite-tantalite, and niobian-tantalian rutile vs. microlite

Microlite is always conspicuously enriched in Ta relative to Nb when compared with coexisting (or replaced) columbite-tantalites and related phases (e.g., Ginsburg, 1956). This is confirmed by all the AC and GL specimens (Fig. 8). Nonequilibrium is indicated by irregular variations in tie-line slopes for identical species pairs, irrespective of the cocrystallization, overgrowth, or replacement relationship.

Compositional data on rutile coexisting with microlite are very scarce. Figure 8 shows microlite to have high Ta/(Ta + Nb) relative to the rutile phase. In contrast, stibiobetafite from its type locality and associated niobian rutile have near-identical Ta/(Ta + Nb); however, stibiobetafite crystallized after and partly at the expense of the niobian rutile (Černý et al., 1979).

Fractionation, contamination, and order-disorder trends

The data from Greer Lake provide ample material for defining the fractionation paths followed by the Nb- and Ta-bearing oxide minerals in the granite and its pegmatite aureole, for considering the possible role of contamination, and for interpreting the pattern of order-disorder relationships.

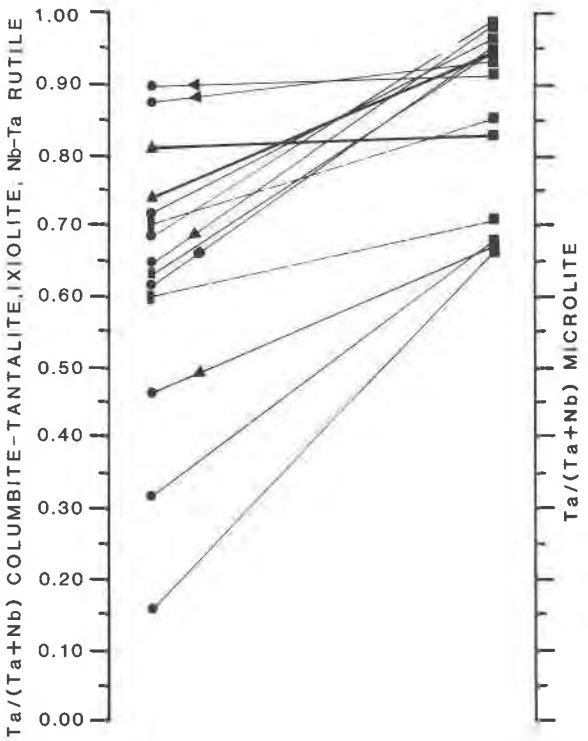

Fig. 8. The atomic Ta/(Ta + Nb) ratios of columbite-tantalites, niobian and tantalian rutiles, and ixiolites related to those of coexisting microlites. Pointed arrowhead on a tie line indicates replacement by microlite; rounded arrowhead marks overgrowth by microlite. Unmarked tie lines indicate cocrystallization of neighboring grains.

Nb/Ta and Fe/Mn fractionation

As shown by Wang et al. (1982), F-based and other complexes of Nb and Ta have different thermal stabilities, the Ta-bearing ones generally persisting to lower temperatures. This could be the principal factor affecting Nb/Ta fractionation in residual granitic and pegmatitic melts. On a local scale of mineral aggregates and individual crystals, the effects of this large-scale mechanism may be augmented by a mass-related difference in diffusion rates, analogous to that proposed for Zr and Hf (Butler and Thompson, 1965).

The fractionation of Fe/Mn is not well understood. On the scale of granitic magma chambers, preferential volatile transfer of Mn was considered by Shaw (1974) and Hildreth (1979, 1981) the only viable mechanism of Fe/Mn separation. Shawe (1968) and Bailey (1977) proposed preferential complexing of Mn with F to explain its separation from Fe and late precipitation.

Fractionation paths of the Greer Lake columbite-tantalites (including the minor ixiolites and wodginites; Fig. 9A) consist of (1) vertical to subvertical segments of pronounced Nb/Ta fractionation at almost constant Mn/(Mn + Fe) and (2) subhorizontal segments marking prominent Fe/Mn fractionation at almost constant Ta/(Ta + Nb).

The Nb/Ta-dominated fractionation is characteristic of internal evolution of the relatively primitive potassic pegmatite phase of the pegmatitic granite and of the less fractionated GL pegmatites (both at Mn/(Mn + Fe) < 0.5). It also marks the internal evolution of the Li- and F-enriched Silverleaf offshoot, the AC2 pod of GRS, and the GL12A pegmatite (at Mn/(Mn + Fe) > 0.8). In contrast, the fractionation segments (or gaps) with dominant shift in Mn/(Mn + Fe) are parallel to major enrichment in Li and F (Figs. 4, 9A): (1) A separate Mn-enriched fractionation trend within the GL group is defined by the 2, 2A, and 11 pegmatites that carry moderate amounts of late Li- and F-enriched muscovite. (2) Another, even more Mn-enriched branch of the GL fractionation seems to be separated from the main two-pronged trend; the GL12A

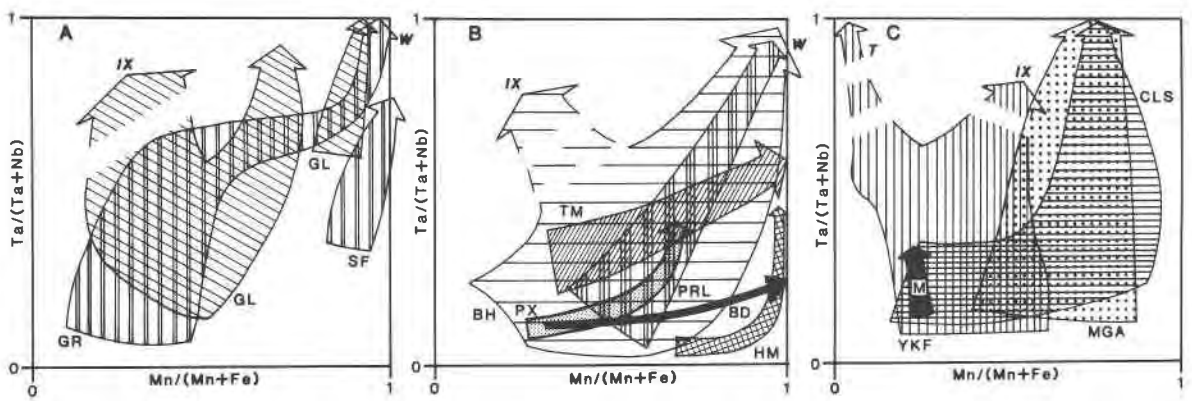

Fig. 9. Fractionation trends of columbite-tantalites in granitic pegmatites, pegmatite groups, and fields, in atomic ratios. Interrupted arrows schematically indicate fractionation gaps between columbite-tantalite proper and ixiolite (IX) or tapiolite (T); W = wodginite. (A) Greer Lake pegmatitic granite and its pegmatite aureole condensed from Figure 4; (B) Black Hills, South Dakota pegmatite field (BH); Tin Mountain (TM) and Peerless (PRL) pegmatites, Black Hills, South Dakota; Plex pegmatite, Baffin Island, N.W.T. (PX); Himalaya pegmatite district, California (HM; Foord 1976); (C) Yellowknife pegmatite field, N.W.T. (YKF) and its Moose pegmatite (M. A. Wise, unpub. ms.); Southern pegmatite series, Cross Lake field, Manitoba (CLS; Anderson, 1984); Mongolian Altai field (MGA; Wang et al., 1981). Nonreferenced trends from unpublished data of P. Černý.

pegmatite contains a lenticular unit of Li- and F-enriched muscovite in its core. (3) A much more enhanced Fe/Mn fractionation is observed at the AC1 locality and particularly in the immediate vicinity of the nearby AC3 pod, which is extremely enriched in Li and F. At this location, the Mn/(Mn + Fe) ratio increases from 0.3–0.5 in the common GRS potassic pegmatite phase to 0.85–1.00 in the AC3 pod, over a distance of only 5 m. (4) The SF aplite-cum-pegmatite offshoot also carries considerable quantities of Li- and F-rich lithian muscovite and lepidolite, and its columbite-tantalites show an isolated fractionation trend at Mn/(Mn + Fe) > 0.84, despite the intermediate 0.36–0.74 range in Ta/(Ta + Nb). A similar relationship is observed in AC2.

The above relationships show that Nb/Ta fractionation can proceed with equal ease in both the primitive, relatively Li- and F-poor magmas and the highly fractionated, Li- and F-saturated melts, reaching the highest levels predominantly (but not exclusively) in the latter. In contrast, Fe/Mn fractionation is greatly enhanced by high activity of F at late stages of granite and/or pegmatite evolution, supporting the idea of F-based complexing of Mn.

Additional evidence for the link between Fe/Mn fractionation and high late-stage a_{F^-} is provided by the columbite-tantalite compositions from other pegmatite localities (Fig. 9B). The Peerless pegmatite (Černý et al., 1985b) and the Tin Mountain deposit of the southern Black Hills, South Dakota are complex pegmatites rich in Li and F, with sizeable concentrations of lithian muscovite in their central parts. Conspicuous Mn-enrichment of Nb- and Ta-bearing oxide minerals occurs at both localities. In the overall fractionation trend of the southern Black Hills field, the Mn-rich side is populated by manganocolumbites and manganotantalites from Li- and F-enriched pegmatites.

Of the other localities shown in Figure 9B, the Himalaya, California, pegmatites (Foord, 1976) and the Brown Derby swarm, Colorado, belong to the lepidolite type of the rare-element pegmatite class; extreme enrichment in Mn precedes most of the Nb/Ta fractionation in their columbite-tantalites. Even the rather primitive, beryl-columbite-type Plex pegmatite (Baffin Island, N.W.T.) shows a prominent Mn-enrichment from the coarse ferrocolumbite crystals of its quartz core to the finer-grained manganocolumbite in late pods of Li- and F-enriched muscovite.

In contrast to the above example, the Yellowknife pegmatite field of the N.W.T. shows an extensive, and locally extreme, Nb/Ta fractionation but restricted Mn/(Mn + Fe) range (0.05–0.45, Fig. 9C; Wise and Černý, 1984b; M. A. Wise, unpub. ms.). This field consists mainly of pegmatites of the beryl-columbite and complex types that lack significant amounts of Li- and F-enriched micas (e.g., the Moose pegmatite, Fig. 9C).

In other cases, the Nb/Ta and Fe/Mn relationships do not lend themselves to unambiguous interpretation. The Southern Series of the Cross Lake field, central Manitoba (Anderson, 1984), shows an early enrichment in Mn followed by extreme Nb/Ta fractionation, from its most primitive biotite-peristerite members to spodumene-rich pegmatites (Fig. 9C); these latter are highly fractionated in terms of all rare-alkali metals, but their mineralogy does not indicate prominent activity of F at any stage of their consolidation. v. Knorring and Fadipe (1981) also indicated manganocolumbite as typical of Li-rich pegmatites, with no reference to a particular role of F. In contrast, the pegmatite field of Mongolian Altai (Wang et al., 1981) does evolve into lepidolite-rich, pollucite- and manganotantalite-bearing pegmatites, but the compositions of columbite from even the most primitive of its members show Mn/(Mn + Fe) > 0.50 (Fig. 9C). Such an example suggests the possibility of Mn-enriched protoliths from which the parent granitic magmas were mobilized, or lithologies through which they passed during their emplacement (e.g., the masutomilite-bearing Tanakamiyama pegmatites in Japan; Harada et al., 1976).

To summarize, Fe/Mn fractionation in columbite-tantalite seems to be greatly enhanced by the high activity of F in late stages of pegmatite consolidation. This may be not the only factor promoting Fe/Mn fractionation, but is evidently the main one responsible for the fractionation pattern in the Greer Lake granite and pegmatite group.

It should be noted here that high activity of F also promotes extreme fractionation of Nb and Ta. Rare-element pegmatites of the lepidolite type carry Ta-rich microlite as their most abundant Nb- and Ta-bearing phase, manganocolumbite being of only minor importance (e.g., the Quartz Creek district, Colorado; Staatz and Trites, 1955). However, widespread as microlite is in the Greer Lake area, it is only a minor phase relative to columbite-tantalite and ixiolite.

Variation in Sn, Ti, and Sc

In the pegmatitic granite, Sn is very low in the primitive potassic pegmatite lenses and the AC pods, but it is enriched in the SF offshoot. In the GL pegmatites, Sn is relatively abundant in the Nb- and Ta-bearing oxide minerals of all paragenetic and geochemical types, and cassiterite is found in some of the more primitive veins (Tables 1–3, Figs. 1, 10). Thus Sn accumulated in the residual fluid phase within the pegmatitic granite and migrated into the pegmatite aureole where it precipitated at presumably lower temperatures. No correlation is apparent between Sn distribution and the rare-alkali or fluorine enrichment of the host assemblages.

Both Ti and Sc are conspicuously low in the orthorhombic Fe-, Mn-, Nb-, and Ta-bearing oxide minerals of the pegmatitic granite assemblages but more abundant in all types of the GL pegmatites (Tables 1–3, Fig. 10). Two interpretations are possible: (1) Ti and Sc could have been complexed and thermally stable in the granite magma and precipitated only at lower temperatures in the pegmatite aureole (as in the thortveitite-bearing, uncontaminated pegmatites hosted by their parent granites at Kobe; Sakurai et al., 1962), or (2) they could have been "absent" from the pristine pegmatitic granite magma and absorbed

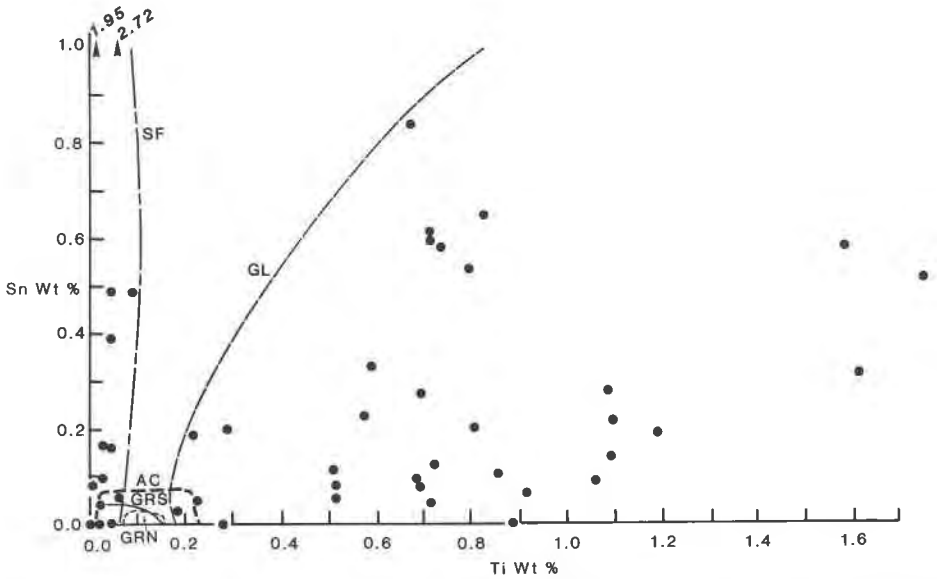

Fig. 10. The Sn and Ti contents of the Greer Lake columbite-tantalites. The GRN, GRS, and AC compositions are represented only by their field boundaries based on 8, 9, and 10 analyses, respectively. Ixiolite data extend the GL field to much higher Sn and Ti values outside this diagram.

by the pegmatite melt only during its passage through metabasaltic country rocks (Norwegian and Madagascar districts as interpreted by Goldschmidt, 1958, and Neumann, 1961). It seems likely that the first mechanism was operative at Greer Lake. However, detailed regional studies of Sc distribution in Nb- and Ta-bearing oxide minerals are virtually nonexistent, and additional data are needed for comparison with pegmatite groups located in diverse host rocks.

Fractionation in columbite-tantalites and garnet

Garnet is the most widespread accessory mineral in the GRN, GRS, AC1, AC3 and GL parageneses; it seems to be missing only in the AC2 pod (Fig. 1). Thus it is of interest to compare the Fe/Mn behavior in columbite-tantalite with that in garnet (Goad and Černý, 1981; Černý et al., 1981a; Goad, 1984). Garnet commonly occurs in several generations in the GL parageneses, and even the

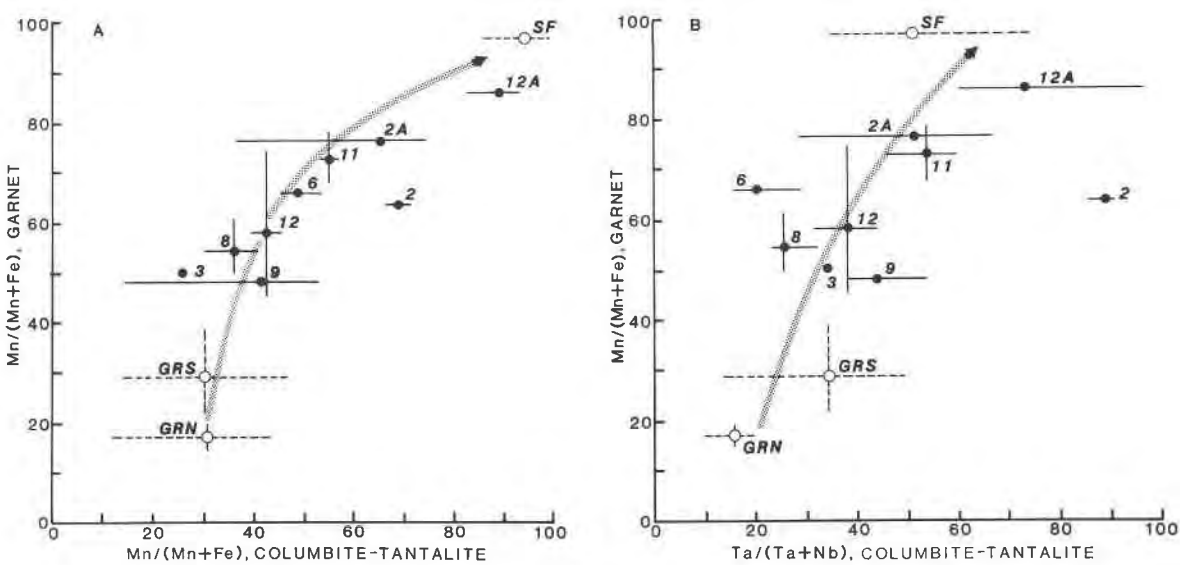

Fig. 11. Correlation of fractionation trends in columbite-tantalite and associated garnet. Data codes correspond to individual locations as shown in Figures 2 and 3.

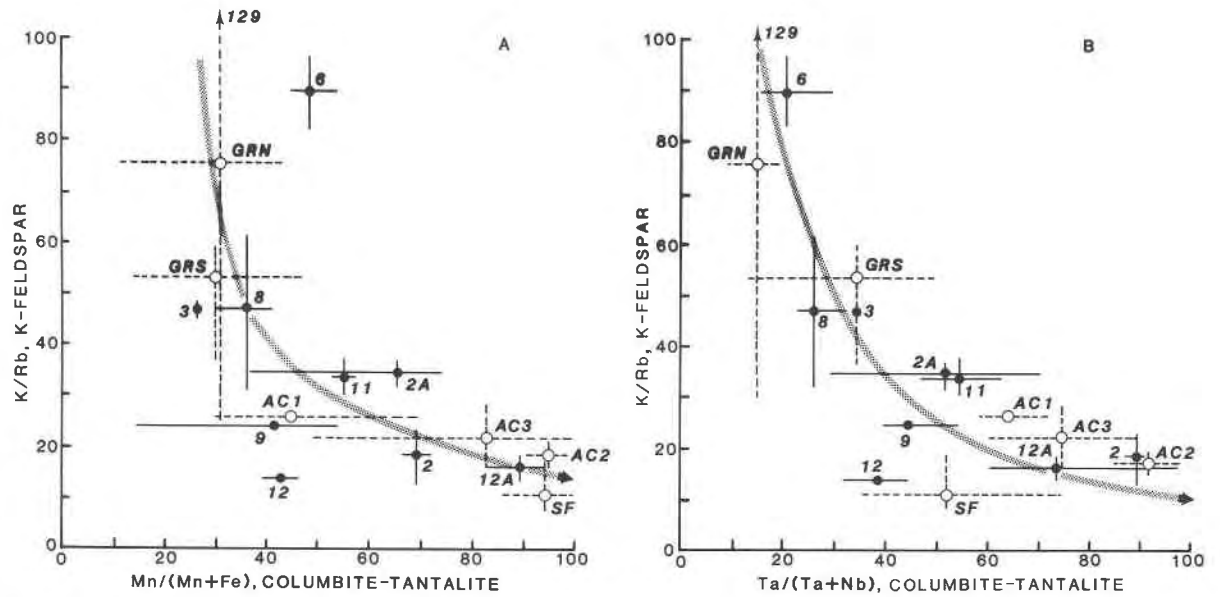

Fig. 12. Correlation of fractionation trends in columbite-tantalite with the K/Rb ratio of blocky, core-margin K-feldspar of parent pegmatites. Data codes correspond to the individual location as shown in Figures 2 and 3.

garnet most closely associated with columbite-tantalite is not found in mutual contact with it. Thus the trend shown in Figure 11A indicates only a correlation of concurrent fractionation paths rather than partition coefficients.

Considering the lack of equilibrium partitioning, the correlation shown in Figure 11A is surprisingly good. The initial rate of Mn enrichment is higher in garnet, whereas columbite-tantalite reaches predominantly manganoan compositions only in the most fractionated pegmatites. Figure 11 shows that the correlation between Mn-enrichment in garnet and Ta-enrichment in columbite-tantalite is rather poor. This is to be expected as Fe/Mn and Nb/Ta trends behave largely independently within the columbite-tantalites themselves (Fig. 4).

Fractionation of columbite-tantalite and K-feldspar

Figure 12 shows the Fe/Mn and Nb/Ta fractionation in columbite-tantalite compared to one of the principal fractionation characteristics of granitic pegmatites, the K/Rb ratio of the core-margin blocky K-feldspar (Goad and Černý, 1981; Černý et al., 1981a; Goad, 1984). Both correlations are rather good: in conjunction with Figure 11, they indicate a concurrent and continual evolution of the Fe/Mn, Nb/Ta, and K/Rb fractionations in the pegmatitic granite and its pegmatite derivatives. Nevertheless, Anderson (1984) showed that this is not always the case and that the degree of correlation may vary rather extensively among different pegmatite groups of the same field (cf. Černý et al., 1985a).

Variation in structural state of columbite-tantalite

The data presented by Černý et al. (1984) and Černý and Ercit (1985) show that partly to largely disordered columbite-tantalites ("pseudo-ixiolites" of Nickel et al., 1963) are more common than largely to completely ordered phases. Two different interpretations are available for the origin of different degrees of ordering in columbite-tantalite. Graham and Thornber (1974) proposed a *sui generis* metamictization, leading to a breakdown of originally homogeneous, compositionally complex phases into submicroscopic intergrowths of several phases of simple stoichiometries; the resulting mixture generates X-ray diffraction patterns of the disordered columbite-tantalite type (cf. Ewing, 1975, and Graham and Thornber, 1975, for discussion). In contrast, experimental evidence indicates that synthetic columbite-tantalites of even the most simple end-member compositions grow initially in the disordered state, attaining partial to complete cation order under extended subsolidus heating. The disordered structure is formed initially as a metastable high-energy arrangement within the stability field of the ordered structure, which subsequently evolves from the disordered state. The disordered structure is more persistent at low T and P, whereas at higher P-T conditions the transition is rapid.

There is a striking relationship between the degree of order in the Greer Lake columbite-tantalites and the distance from the pegmatitic granite intrusion (Figs. 3, 6). Within the pegmatitic granite, the GRN, GRS, and AC columbite-tantalites show intermediate to considerably ordered structures; the nearby SF offshoot shows a range of disordered to considerably ordered phases, and the GL pegmatites carry highly disordered columbite-tantalites. Such a distribution of structural states may have been controlled by differences in postcrystallization cooling rates, in accord with the experimental evidence quoted above. Assuming initial crystallization of all columbite-tantalites in the disordered state, conditions of relatively fast cooling in the small and dispersed GL pegmatites

would lead to metastable preservation of disorder, whereas longer periods of higher T in the slow-cooling large mass of the pegmatitic granite would promote ordering. The SF columbite-tantalites would represent an intermediate case. An analogy to the distribution pattern of order-disorder in columbite-tantalite is shown by the wodginite-ixiolite pair: relatively ordered wodginite occurs within the pegmatitic granite, but the disordered ixiolites occur only in the aureole of pegmatite veins.

The above interpretation may be oversimplified, and it is not necessarily applicable to other localities. For example, manganotantalites tend to be either highly ordered or highly disordered (Černý and Ercit, 1985); thus the structural state of the SF manganocolumbites-manganotantalites may be subject to a specific crystallochemical control. Electrostatic energy calculations of Giese (1975) suggest that manganocolumbites of different structural states may originate with about equal ease, because of minimal energetic differences between the different cation arrangements. Consequently, the structural state may easily be affected by other factors. The most obvious is compositional variation disturbing the stoichiometry. It was noted earlier that the GL columbite-tantalites contain Sn, Ti, and Sc distinctly above their concentration in the GRN, GRS, and AC and partly in the SF specimens. Thus it is possible that the presence of R^{3+} and R^{4+} cations in the structure may have been an important factor in preventing the GL columbite-tantalites from even incipient ordering.

Concluding remarks

Fractionation of Fe/Mn and Nb/Ta in the Nb- and Ta-bearing oxide minerals of the Greer Lake granite-pegmatite sequence evolves with the general fractionation characteristics of these rocks, as exemplified by the Mn enrichment in garnet and the increase in rare alkali metals in K-feldspar. However, the Nb/Ta fractionation proceeds at similar rates in all environments whereas Mn enrichment is particularly enhanced by high activity of F. Preferential concentration of Sn occurs in the pegmatite aureole, but the mechanism of this is not understood. Enrichment of Ti and Sc in the Nb- and Ta-bearing oxide minerals of the pegmatites seems to be due to primary fractionation of these elements into the highly evolved pegmatite melts, rather than to assimilation from metabasaltic country rocks. The order-disorder relationships in columbite-tantalite, wodginite, and ixiolite together with their distribution in the different units suggests crystallization of all these phases in the disordered state; subsequent partial ordering proceeds in the solid state, at rates inverse to those of the cooling of the parent rock. However, the degree of disorder also shows positive correlation with Ti, Sn, Fe^{3+}, and Sc, and the possibility of a crystallochemical control of the structural state cannot be dismissed.

The paragenesis and geochemical evolution of Nb- and Ta-bearing oxide minerals in granitic pegmatites should be examined by experimental modeling and painstaking studies of natural assemblages. The experimental approach should address (1) Fe, Mn, Nb, Ta, Sn, Ti, and Sc speciation and mobility in pegmatite melts and fluids; (2) the role of F in Fe/Mn fractionation; (3) ixiolite stability, as opposed to that of wodginite, tapiolite + cassiterite + columbite-tantalite, tapiolite + rutile + columbite-tantalite, and other relevant assemblages; and (4) order-disorder in synthetic columbite-tantalite and wodginite-ixiolite, under conditions close to those of granitic pegmatite crystallization.

Thorough studies are required of the paragenesis, composition, structural state and mutual relationships of complete assemblages of Nb- and Ta-bearing oxide minerals from individual pegmatites and from parental granitoids plus their pegmatite aureoles. Particular attention should be paid to selecting geologically well-characterized pegmatites and pegmatite groups characteristic of different classes and types. In order to fully exploit recent advances in crystal chemistry of the Nb-, Ta-, Ti-, and Sn-bearing oxide minerals in a geologic context, complete structural, chemical, and paragenetic information on the oxide and coexisting silicate minerals is required; such essential information is currently scarce.

Acknowledgments

The authors are indebted to T. S. Ercit and to E. E. Foord for providing some of the electron-microprobe and structural data used in this study and for critical reviews of an early draft of the manuscript. Karen J. Ferreira and Len Chackowsky provided extensive help in the X-ray diffraction studies. T. S. Ercit made some of his unpublished data available and developed some of the methods of formula calculation. D. L. Trueman, Reijo Alviola, and Lance Barber were of valuable assistance in the field. This work was supported by the NSERC of Canada Operating Grants to Černý and Hawthorne, by a University Research Fellowship to Hawthorne, by the DEMR Research Agreements with Černý; by the Canada-Manitoba Subsidiary Agreement on Mineral Exploration subcontracted in part to Černý; and by the logistic support and research grants from the Tantalum Mining Corporation of Canada, Ltd. to Černý.

References

Anderson, A.J. (1984) Geochemistry, mineralogy and petrology of the Cross Lake pegmatite field, Manitoba. M.Sc. thesis, University of Manitoba, Winnipeg.

Appleman, D. E., and Evans, H.T., Jr. (1973) Job 9214: Indexing and least-squares refinement of powder diffraction data. U.S. Geological Survey Computer Contributions 20; NTIS Document PB2-16188.

Bailey, J.C. (1977) Fluorine in granitic rocks and melts: A review. Chemical Geology, 19, 1–42.

Beus, A.A. (1960) Geochemistry of beryllium and genetic types of beryllium deposits. (in Russian) Academy of Sciences USSR, Moscow (transl. Freeman and Co., 1966).

Borisenko, L.F., Maximova, N.V., and Kazakova, M.Ye. (1969) Scandian ixiolite, a new tantalo-niobate species with formula $(A,B)_nO_{2n}$. (in Russian) Academy of Sciences USSR Doklady, 189, 148–151.

Butler, J.R., and Thompson, A.J. (1965) Zirconium:hafnium ratio in some igneous rocks. Geochimica et Cosmochimica Acta, 29, 167–175.

Černý, Petr. (1982) Anatomy and classification of granitic pegmatites. In P. Černý, Ed. Granitic pegmatites in science and

industry, 1–39. Mineralogical Association of Canada Short Course Handbook 8.
Černý, Petr, and Ercit, T.S. (1985) Some recent advances in the mineralogy and geochemistry of Nb and Ta in rare-element granitic pegmatites. Bulletin de Minéralogie, 108, 499–532.
Černý, Petr, and Turnock, A.C. (1971) Niobium-tantalum minerals from granitic pegmatites at Greer Lake, southeastern Manitoba. Canadian Mineralogist, 10, 755–772.
Černý, Petr, Hawthorne, F.C., Laflamme, J.H.G., and Hinthorne, James. (1979) Stibiobetafite, a new member of the pyrochlore group from Věžná, Czechoslovakia. Canadian Mineralogist, 17, 583–588.
Černý, Petr, Trueman, D.L., Ziehlke, D.V., Goad, B.E., and Paul, B.J. (1981a) The Cat Lake–Winnipeg River and Wekusko Lake pegmatite fields, Manitoba. Manitoba Mineral Resources Division, Economic Geology Report, ER80-1.
Černý, Petr, Paul, B.J., Hawthorne, F.C., and Chapman, Ronald. (1981b) A niobian rutile–disordered columbite intergrowth from the Huron Claim pegmatite, southeastern Manitoba. Canadian Mineralogist, 19, 541–548.
Černý, Petr, Ercit, T.S., and Wise, M.A. (1984) Compositional and structural variability in columbite-tantalite and tapiolite. Geological Society of America Abstracts with Programs, 16, 466.
Černý, Petr, Meintzer, R. E., and Anderson, A.J. (1985a) Extreme fractionation in rare-element granitic pegmatites: Selected examples of data and mechanisms. Canadian Mineralogist, 23, 381–421.
Černý, Petr, Roberts, W.L., Ercit, T.S., and Chapman, Ronald. (1985b) Wodginite and associated minerals from the Peerless pegmatite, Pennington County, South Dakota. American Mineralogist, 70, 1044–1049.
Colby, J.W. (1980) MAGIC V—A computer program for quantitative electron-excited energy dispersive analysis. In QUANTEX-RAY Instructional Manual, KEVEX Corporation, Foster City, California.
Ercit, T.S. (1985) The simpsonite paragenesis: The crystal chemistry and geochemistry of extreme tantalum fractionation. Ph.D. thesis, University of Manitoba, Winnipeg.
Ercit, T.S., Černý, Petr, and Hawthorne, F.C. (1984) The crystal chemistry of wodginite. Geological Society of America Abstracts with Programs, 16, 502.
——— (1985) Normal and inverse pyrochlore group minerals. Geological Association of Canada–Mineralogical Association of Canada, Abstracts with Programs, 10, A17.
Ewing, R.C. (1975) The crystal chemistry of complex niobium and tantalum oxides: IV. The metamict state. Discussion. American Mineralogist, 60, 728–733.
Ferreira, K.J. (1984) The mineralogy and geochemistry of the Lower Tanco pegmatite, Bernic Lake, Manitoba, Canada. M.Sc. thesis, University of Manitoba, Winnipeg.
Foord, E.E. (1976) Mineralogy and petrogenesis of layered pegmatite-aplite dikes in the Mesa Grande district, San Diego County, California. Ph.D. thesis, Stanford University, Stanford, California.
——— (1982) Minerals of Sn, Ti, Nb and Ta in granitic pegmatites. In P. Černý, Ed. Granitic pegmatites in science and industry, 187–238. Mineralogical Association of Canada Short Course Handbook 8.
Giese, R.F., Jr. (1975) Electrostatic energy of columbite-ixiolite. Nature, 256, 31–32.
Ginsburg, A.I. (1956) On some characteristics of tantalum geochemistry and on the types of tantalum mineralization. (in Russian) Geokhimiya, 74–83.
Goad, B.E. (1984) Pegmatitic granites from the Winnipeg River district, southeastern Manitoba. M.Sc. thesis, University of Manitoba, Winnipeg.
Goad, B.E., and Černý, Petr. (1981) Peraluminous pegmatitic granites and their pegmatite aureoles in the Winnipeg River district, southeastern Manitoba. Canadian Mineralogist, 19, 177–194.
Goldschmidt, V.M. (1958) Geochemistry. A. Muir, Ed., Oxford University Press.
Graham, James, and Thornber, M.R. (1974) The crystal chemistry of complex niobium and tantalum oxides: IV. The metamict state. American Mineralogist, 59, 1047–1050.
——— (1975) The crystal chemistry of complex niobium and tantalum oxides: IV. The metamict state. Reply. American Mineralogist, 60, 734.
Grice, J.D., Černý, Petr, and Ferguson, R.B. (1972) The Tanco pegmatite at Bernic Lake, Manitoba. II. Wodginite, tantalite, pseudo-ixiolite and related minerals. Canadian Mineralogist, 11, 609–642.
Harada, Kazuo, Honda, M., Nagashima, Kozo, and Kanisawa, Satoshi. (1976) Masutomilite, manganese analogue of zinnwaldite, with special reference to masutomilite-lepidolite-zinnwaldite series. Mineralogical Journal Japan, 8, 95–109.
Hildreth, Wes. (1979) The Bishop tuff: Evidence for the origin of compositional zonation in silicic magma chambers. Geological Society of America Special Paper 180, 43–75.
——— (1981) Gradients in silicic magma chambers: Implications for lithospheric magmatism. Journal of Geophysical Research, 86, B11, 10153–10192.
Khvostova, V.A., Lebedeva, S.I., and Maksimova, N.V. (1983) Tin-bearing tantaloniobates and their typomorphic features. Rare minerals of the tin-bearing tantaloniobate group. International Geology Review, 922–932.
v. Knorring, Oleg, and Condliffe, E. (1984) On the occurrence of niobium, tantalum, and other rare element minerals in Meldon aplite, Devonshire. Mineralogical Magazine, 48, 443–448.
v. Knorring, Oleg, and Fadipe, Akinola. (1981) On the mineralogy and geochemistry of niobium and tantalum in some granite pegmatites and alkali granites of Africa. Bulletin de Minéralogie, 104, 496–507.
v. Knorring, Oleg, Sahama, Th.G., and Lehtinen, Martti. (1969) Scandian ixiolite from Mozambique and Madagascar. Geological Society of Finland Bulletin, 41, 75–77.
Komkov, A.I. (1970) Relationship between the X-ray constants of columbites and composition. (in Russian) Academy of Sciences USSR Doklady, 195, 434–436.
Kuzmenko, M.V. (1978) Geochemistry of tantalum and genesis of endogenous tantalum deposits. (in Russian) Nauka, Moscow.
Lahti, Seppo (1984) The composition field of some Nb-Ta minerals in pegmatites—New observations. 27th International Geological Congress, Abstracts 5, sections 10 and 11, 92–93.
Longstaffe, F.J., Černý, Petr, and Muehlenbachs, K. (1981) Oxygen isotope geochemistry of the granitoids in the Winnipeg River pegmatite district, southeastern Manitoba. Canadian Mineralogist, 19, 195–204.
Lumpkin, G.R., Chakoumakos, B.C., and Ewing, R.C. (1986) Mineralogy and radiation effects of microlite from the Harding pegmatite, Taos County, New Mexico. American Mineralogist, 71, 569–588.
Neumann, H. (1961) The scandium content of some Norwegian minerals and the formation of thortveitite, a reconnaissance survey. Norsk Geologisk Tiddskrift, 41, 197–210.
Nickel, E.H., Rowland, J.F., and McAdam, R.C. (1963) Ixiolite, a columbite substructure. American Mineralogist, 48, 961–979.
Paul, B.J. (1984) Mineralogy and geochemistry of the Huron Claim pegmatite, southeastern Manitoba. M.Sc. thesis, University of Manitoba, Winnipeg.
Rucklidge, John, and Gasparrini, Elvira. (1969) Electron microprobe analytical data reduction (EMPADR VII). Department of Geology, University of Toronto.
Sahama, Th.G. (1980) Minerals of the tantalite-niobite series from Mozambique. Bulletin de Minéralogie, 103, 190–197.
Sakurai, Kin-ichi, Nagashima, K., and Kato, Akira. (1962) Thortveitite from Kobe, Omiya, Kyoto, Japan. Chemical Society of Japan Bulletin, 35, 1776–1779.
Shaw, H.R. (1974) Diffusion of H_2O in granitic liquids. In A.W.

Hoffman et al., Eds. Geochemical transport and kinetics, 139–170. Carnegie Institution of Washington Publication 634.

Shawe, D.R. (1968) Geology of the Spor Mountain beryllium district, Utah. In J.D. Ridge, Ed. Ore deposits in the United States, 1933–1967, 2, 1148–1161. AIMMPE, New York.

Solodov, N.A. (1971) Scientific principles of perspective evaluation of rare-element pegmatites. (in Russian) Nauka, Moscow.

Staatz, M.H., and Trites, A.F. (1955) Geology of the Quartz Creek pegmatite district, Gunnison County, Colorado. U.S. Geological Survey Professional Paper 265.

Trueman, D.L. (1980) Stratigraphic, structural and metamorphic petrology of the Archean greenstone belt at Bird River, Manitoba. Ph.D. thesis, University of Manitoba, Winnipeg.

Wang, X.-J., Zou, T.-R., Xu, J.-G., Yu, X.-Y., and Qiu, Y.-Zh. (1981) Study of pegmatite minerals of the Altai region. (in Chinese) Science Publishing House, Beijing.

Wang, Y.-R., Li, J.-T., Lu, J.-L., and Fan, W.-L. (1982) Geochemical mechanism of Nb-Ta mineralization during the late stage of granite crystallization. Geochemistry (Beijing), 1, 175–185.

Weitzel, H. (1976) Kristallstrukturverfeinerung von Wolframiten und Columbiten. Zeitschrift für Kristallographie, 144, 238–258.

Wise, M.A., and Černý, Petr. (1984a) First U.S. occurrence of wodginite from Powhatan County, Virginia. American Mineralogist, 69, 807–809.

——— (1984b) Geochemistry of Nb-Ta-Sn minerals from the Yellowknife pegmatite field, N.W.T. Geological Society of America Abstracts with Programs, 16, 699.

Wise, M.A., Turnock, A.C., and Černý, Petr. (1985) Improved unit cell dimensions for ordered columbite-tantalite end-members. Neues Jahrbuch für Mineralogie, Monatshefte, 1985, 372–378.

Manuscript received February 28, 1985
Manuscript accepted October 1, 1985